Zhang, R. "Seismic Isolation and Supplemental Energy Dissipation."
*Bridge Engineering Handbook.*
Ed. Wai-Fah Chen and Lian Duan
Boca Raton: CRC Press, 2000

# 41

# Seismic Isolation and Supplemental Energy Dissipation




Rihui Zhang
*California State Department of Transportation*


## 41.1 Introduction

Strong earthquakes impart substantial amounts of energy into structures and may cause the structures to deform excessively or even collapse. In order for structures to survive, they must have the capability to dissipate this input energy through either their inherent damping mechanism or inelastic deformation. This issue of energy dissipation becomes even more acute for bridge structures because most bridges, especially long-span bridges, possess very low inherent damping, usually less than 5% of critical. When these structures are subjected to strong earthquake motions, excessive deformations can occur by relying on only inherent damping and inelastic deformation. For bridges designed mainly for gravity and service loads, excessive deformation leads to severe damage or even collapse. In the instances of major bridge crossings, as was the case of the San Francisco–Oakland

Bay Bridge during the 1989 Loma Prieta earthquake, even noncollapsing structural damage may cause very costly disruption to traffic on major transportation arteries and is simply unacceptable.

Existing bridge seismic design standards and specifications are based on the philosophy of accepting minor or even major damage but no structural collapse. Lessons learned from recent earthquake damage to bridge structures have resulted in the revision of these design standards and a change of design philosophy. For example, the latest bridge design criteria for California [1] recommend the use of a two-level performance criterion which requires that a bridge be designed for both safety evaluation and functional evaluation design earthquakes. A safety evaluation earthquake event is defined as an event having a very low probability of occurring during the design life of the bridge. For this design earthquake, a bridge is expected to suffer limited significant damage, or immediately repairable damage. A functional evaluation earthquake event is defined as an event having a reasonable probability of occurring once or more during the design life of the bridge. Damages suffered under this event should be immediately repairable or immediate minimum for important bridges. These new criteria have been used in retrofit designs of major toll bridges in the San Francisco Bay area and in designs of some new bridges. These design criteria have placed heavier emphasis on controlling the behavior of bridge structural response to earthquake ground motions.

For many years, efforts have been made by the structural engineering community to search for innovative ways to control how earthquake input energy is absorbed by a structure and hence controlling its response to earthquake ground motions. These efforts have resulted in the development of seismic isolation techniques, various supplemental energy dissipation devices, and active structural control techniques. Some applications of these innovative structural control techniques have proved to be cost-effective. In some cases, they may be the only ways to achieve a satisfactory solution. Furthermore, with the adoption of new performance-based design criteria, there will soon come a time when these innovative structural control technologies will be the choice of more structural engineers because they offer economical alternatives to traditional earthquake protection measures.

Topics of structural response control by passive and active measures have been covered by several authors for general structural applications [2–4]. This chapter is devoted to the developments and applications of these innovative technologies to bridge structures. Following a presentation of the basic concepts, modeling, and analysis methods, brief descriptions of major types of isolation and energy dissipation devices are given. Performance and testing requirements will be discussed followed by a review of code developments and design procedures. A design example will also be given for illustrative purposes.

## 41.2 Basic Concepts, Modeling, and Analysis

The process of a structure responding to earthquake ground motions is actually a process involving resonance buildup to some extent. The severity of resonance is closely related to the amount of energy and its frequency content in the earthquake loading. Therefore, controlling the response of a structure can be accomplished by either finding ways to prevent resonance from building up or providing a supplemental energy dissipation mechanism, or both. Ideally, if a structure can be separated from the most-damaging energy content of the earthquake input, then the structure is safe. This is the idea behind seismic isolation. An isolator placed between the bridge superstructure and its supporting substructure, in the place of a traditional bearing device, substantially lengthens the fundamental period of the bridge structure such that the bridge does not respond to the most-damaging energy content of the earthquake input. Most of the deformation occurs across the isolator instead of in the substructure members, resulting in lower seismic demand for substructure members. If it is impossible to separate the structure from the most-damaging energy content, then the idea of using supplemental damping devices to dissipate earthquake input energy and to reduce structural damage becomes very attractive.

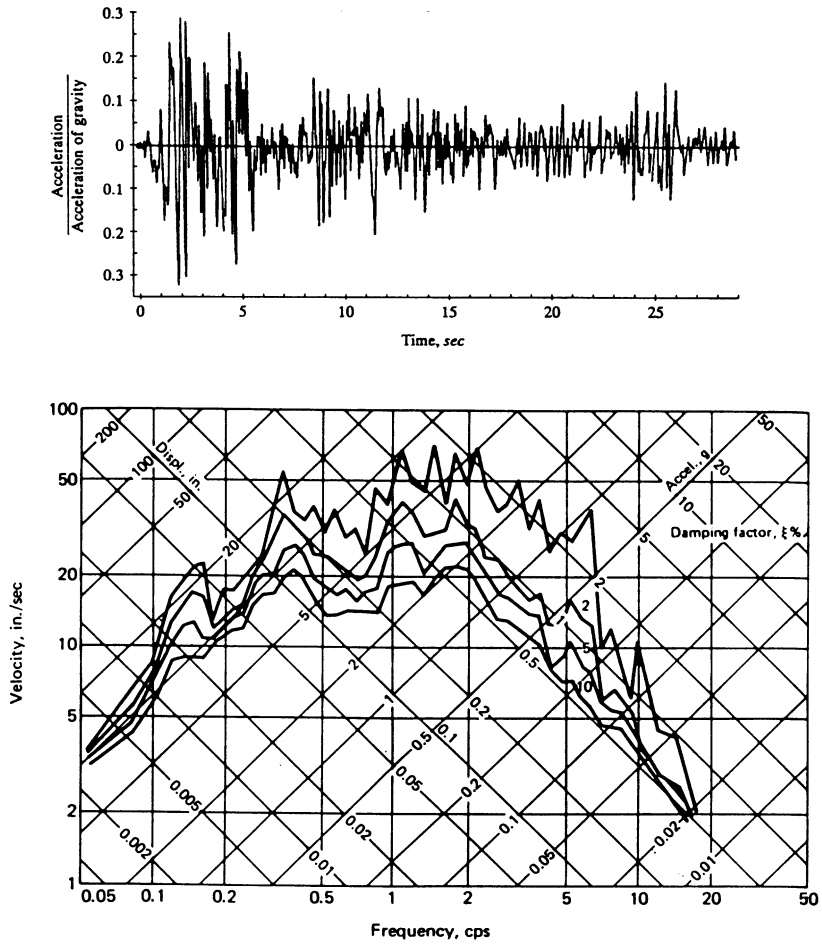


**FIGURE 41.1** Acceleration time history and response spectra from El Centro earthquake, May 1940.

In what follows, theoretical basis and modeling and analysis methods will be presented mainly based on the concept of earthquake response spectrum analysis.

## 41.2.1 Earthquake Response Spectrum Analysis

Earthquake response spectrum analysis is perhaps the most widely used method in structural earthquake engineering design. In its original definition, an earthquake response spectrum is a plot of the maximum response (maximum displacement, velocity, acceleration) to a specific earthquake ground motion for all possible single-degree-of-freedom (SDOF) systems. One of such response spectra is shown in Figure 41.1 for the 1940 El Centro earthquake. A response spectrum not only reveals how systems with different fundamental vibration periods respond to an earthquake ground motion, when plotted for different damping values, site soil conditions and other factors, it also shows how these factors are affecting the response of a structure. From an energy point of view, response spectrum can also be interpreted as a spectrum the energy frequency contents of an earthquake.

Since earthquakes are essentially random phenomena, one response spectrum for a particular earthquake may not be enough to represent the earthquake ground motions a structure may

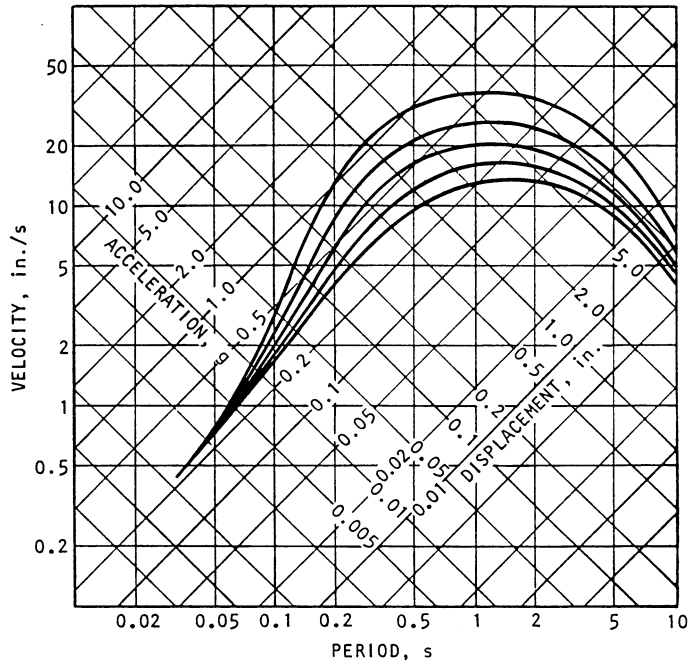


**FIGURE 41.2** Example of smoothed design spectrum.

experience during its service life. Therefore, the design spectrum, which incorporates response spectra for several earthquakes and hence represents a kind of "average" response, is generally used in seismic design. These design spectra generally appear to be smooth or to consist of a series of straight lines. Detailed discussion of the construction and use of design spectra is beyond the scope of this chapter; further information can be found in References [5,6]. It suffices to note for the purpose of this chapter that design spectra may be used in seismic design to determine the response of a structure to a design earthquake with given intensity (maximum effective ground acceleration) from the natural period of the structure, its damping level, and other factors. Figure 41.2 shows a smoothed design spectrum curve based on the average shapes of response spectra of several strong earthquakes.

### 41.2.2 Structural Dynamic Response Modifications

By observing the response/design spectra in Figures 41.1a, it is seen that manipulating the natural period and/or the damping level of a structure can effectively modify its dynamic response. By inserting a relatively flexible isolation bearing in place of a conventional bridge bearing between a bridge superstructure and its supporting substructure, seismic isolation bearings are able to lengthen the natural period of the bridge from a typical value of less than 1 second to 3 to 5 s. This will usually result in a reduction of earthquake-induced response and force by factors of 3 to 8 from those of fixed-support bridges [7].

As for the effect of damping, most bridge structures have very little inherent material damping, usually in the range of 1 to 5% of critical. The introduction of nonstructural damping becomes necessary to reduce the response of a structure.

Some kind of a damping device or mechanism is also a necessary component of any successful seismic isolation system. As mentioned earlier, in an isolated structural system deformation mainly occurs across the isolator. Many factors limit the allowable deformation taking place across an

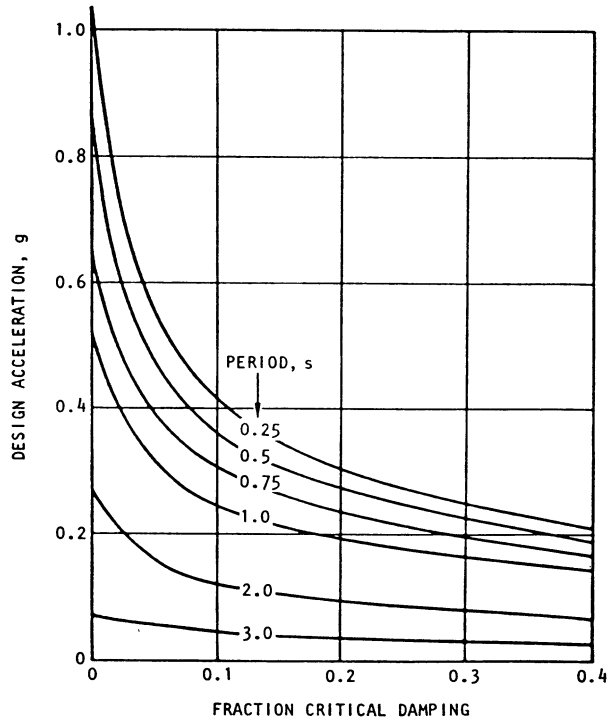


**FIGURE 41.3** Effect of damping on response spectrum.

isolator, e.g., space limitation, stability requirement, etc. To control deformation of the isolators, supplemental damping is often introduced in one form or another into isolation systems.

It should be pointed out that the effectiveness of increased damping in reducing the response of a structure decreases beyond a certain damping level. Figure 41.3 illustrates this point graphically. It can be seen that, although acceleration always decreases with increased damping, its rate of reduction becomes lower as the damping ratio increases. Therefore, in designing supplemental damping for a structure, it needs to be kept in mind that there is a most-cost-effective range of added damping for a structure. Beyond this range, further response reduction will come at a higher cost.

### 41.2.3 Modeling of Seismically Isolated Structures

A simplified SDOF model of a bridge structure is shown in Figure 41.4. The mass of the superstructure is represented by $m$, pier stiffness by spring constant $k_0$, and structural damping by a viscous damping coefficient $c_0$. The equation of motion for this SDOF system, when subjected to an earthquake ground acceleration excitation, is expressed as:

$$m_0\ddot{x} + c_0\dot{x} + k_0 x = -m_0\ddot{x}_g \tag{41.1}$$

The natural period of motion $T_0$, time required to complete one cycle of vibration, is expressed as

$$T_0 = 2\pi\sqrt{\frac{m_0}{k_0}} \tag{41.2}$$

Addition of a seismic isolator to this system can be idealized as adding a spring with spring constant $k_i$ and a viscous damper with damping coefficient $c_i$, as shown in Figure 41.5. The combined stiffness of the isolated system now becomes

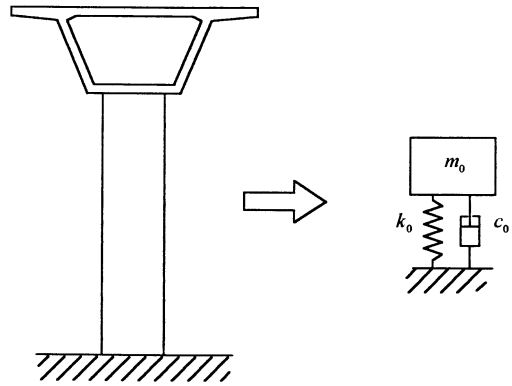


**FIGURE 41.4** SDOF dynamic model.

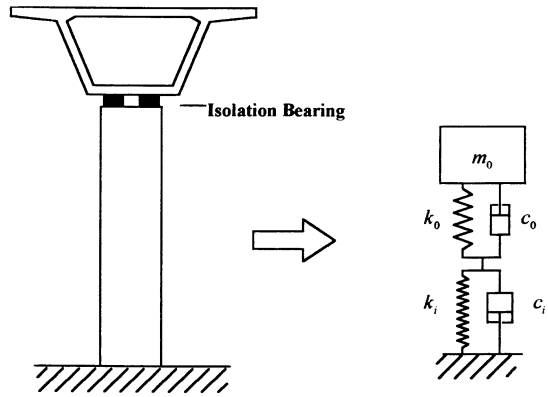


**FIGURE 41.5** SDOF system with seismic isolator.

$$K = \frac{k_0 k_i}{k_0 + k_i} \tag{41.3}$$

Equation (41.1) is modified to

$$m_0\ddot{x} + \left(c_0 + c_i\right)\dot{x} + Kx = -m_0\ddot{x}_g \tag{41.4}$$

and the natural period of vibration of the isolated system becomes

$$T = 2\pi\sqrt{\frac{m_0}{K}} = 2\pi\sqrt{\frac{m_0\left(k_0 + k_i\right)}{k_0 k_i}} \tag{41.5}$$

When the isolator stiffness is smaller than the structural stiffness, $K$ is smaller than $k_0$; therefore, the natural period of the isolated system $T$ is longer than that of the original system. It is of interest to note that, in order for the isolator to be effective in modifying the the natural period of the structure, $k_i$ should be smaller than $k_0$ to a certain degree. For example, if $k_i$ is 50% of $k_0$, then $T$ will be about 70% larger than $T_0$. If $k_i$ is only 10% of $k_0$, then $T$ will be more than three times of $T_0$.

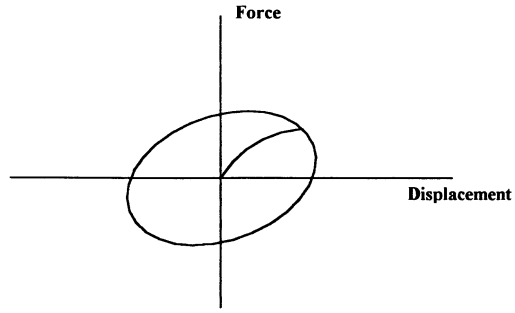


**FIGURE 41.6** Generic damper hysteresis loops.

More complex structural systems will have to be treated as multiple-degree-of-freedom (MDOF) systems; however, the principle is the same. In these cases, spring elements will be added to appropriate locations to model the stiffness of the isolators.

### 41.2.4 Effect of Energy Dissipation on Structural Dynamic Response

In discussing energy dissipation, the terms *damping* and *energy dissipation* will be used interchangeably. Consider again the simple SDOF system used in the previous discussion. In the theory of structural dynamics [8], critical value of damping coefficient $c_c$ is defined as the amount of damping that will prevent a dynamic system from free oscillation response. This critical damping value can be expressed in terms of the system mass and stiffness:

$$c_c = 2\sqrt{m_0 k_o} \tag{41.6}$$

With respect to this critical damping coefficient, any amount of damping can now be expressed in a relative term called damping ratio $\xi$, which is the ratio of actual system damping coefficient over the critical damping coefficient. Thus,

$$\xi = \frac{c_0}{c_c} = \frac{c_0}{2\sqrt{m_0 k_0}} \tag{41.7}$$

Damping ratio is usually expressed as a percentage of the critical. With the use of damping ratio, one can compare the amount of damping of different dynamic systems.

Now consider the addition of an energy dissipation device. This device generates a force $f(x, \dot{x})$ that may be a function of displacement or velocity of the system, depending on the energy dissipation mechanism. Figure 41.6 shows a hysteresis curve for a generic energy dissipation device. Equation (41.1) is rewritten as

$$x + \frac{c_0}{m_0}x + \frac{k_0}{m_0}x + \frac{f(x,x)}{m_0} = -x_g \tag{41.8}$$

There are different approaches to modeling the effects damping devices have on the dynamic response of a structure. The most accurate approach is linear or nonlinear time history analysis by modeling the true behavior of the damping device. For practical applications, however, it will often be accurate enough to represent the effectiveness of a damping mechanism by an equivalent viscous damping ratio. One way to define the equivalent damping ratio is in terms of energy $E_d$ dissipated

by the device in one cycle of cyclic motion over the maximum strain energy $E_{ms}$ stored in the structure [8]:

$$\xi_{eq} = \frac{E_d}{4_\pi E_{ms}} \tag{41.9}$$

For a given device, $E_d$ can be found by measuring the area of the hysteresis loop. Equation (41.9) can now be rewritten by introducing damping ratio $\xi_0$ and $\xi_{eq}$, in the form

$$\ddot{x} + 2\sqrt{\frac{k_0}{m}}\left(\xi + \xi_{eq}\right)\dot{x} + \frac{k_0}{m_0}x = -\ddot{x}_g \tag{41.10}$$

This concept of equivalent viscous damping ratio can also be generalized to use for MDOF systems by considering $\xi_{eq}$ as modal damping ratio and $E_d$ and $E_{ms}$ as dissipated energy and maximum strain energy in each vibration mode [9]. Thus, for the $i$th vibration mode of a structure, we have

$$\xi_{eq}^{i} = \frac{E_d^i}{4\pi E_{ms}^i} \tag{41.11}$$

Now the dynamic response of a structure with supplemental damping can be solved using available linear analysis techniques, be it linear time history analysis or response spectrum analysis.

## 41.3 Seismic Isolation and Energy Dissipation Devices

Many different types of seismic isolation and supplemental energy dissipation devices have been developed and tested for seismic applications over the last three decades, and more are still being investigated. Their basic behaviors and applications for some of the more widely recognized and used devices will be presented in this section.

### 41.3.1 Elastomeric Isolators

Elastomeric isolators, in their simplest form, are elastomeric bearings made from rubber, typically in cylindrical or rectangular shapes. When installed on bridge piers or abutments, the elastomeric bearings serve both as vertical bearing devices for service loads and lateral isolation devices for seismic load. This requires that the bearings be stiff with respect to vertical loads but relatively flexible with respect to lateral seismic loads. In order to be flexible, the isolation bearings have to be made much thicker than the elastomeric bearing pads used in conventional bridge design. Insertion of horizontal steel plates, as in the case of steel reinforced elastomeric bearing pads, significantly increases vertical stiffness of the bearing and improves stability under horizontal loads. The total rubber thickness influences essentially the maximum allowable lateral displacement and the period of vibration.

For a rubber bearing with given bearing area $A$, shear modulus $G$, height $h$, allowable shear strain $\gamma$, shape factor $S$, and bulk modulus $K$, its horizontal stiffness and period of vibration can be expressed as

$$K = \frac{GA}{h} \tag{41.12}$$

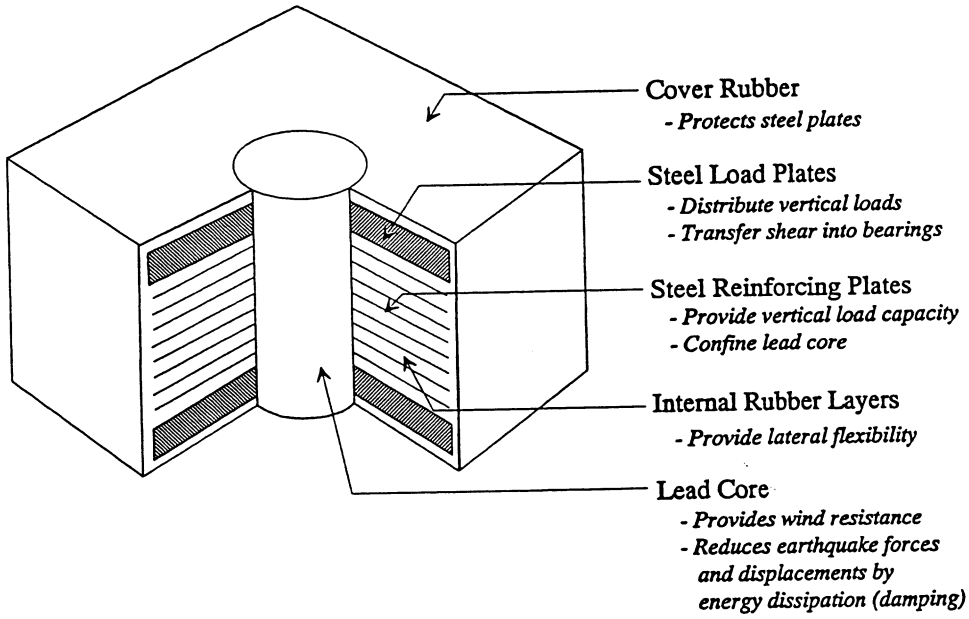


**FIGURE 41.7** Typical construction of a lead core rubber bearing.

$$T_b = 2\pi\sqrt{\frac{M}{K}} = 2\pi\sqrt{\frac{Sh\gamma A'}{Ag}} \tag{41.13}$$

where $A'$ is the overlap of top and bottom areas of a bearing at maximum displacement. Typical values for bridge elastomeric bearing properties are $G = 1$ MPa (145 psi), $K = 200$ MPa (290 psi), $\gamma = 0.9$ to 1.4, $S = 3$ to 40. The major variability lies in $S$, which is a function of plan dimension and rubber layer thickness.

One problem associated with using pure rubber bearings for seismic isolation is that the bearing could easily experience excessive deformation during a seismic event. This will, in many cases, jeopardize the stability of the bearing and the superstructure it supports. One solution is to add an energy dissipation device or mechanism to the isolation bearing. The most widely used energy dissipation mechanism in elastomeric isolation bearing is the insertion of a lead core at the center of the bearing. Lead has a high initial shear stiffness and relatively low shear yielding strength. It essentially has elastic–plastic behavior with good fatigue properties for plastic cycles. It provides a high horizontal stiffness for service load resistance and a high energy dissipation for strong seismic load, making it ideal for use with elastomeric bearings.

This type of lead core elastomeric isolation, also known as lead core rubber bearing (LRB), was developed and patented by the Dynamic Isolation System (DIS). The construction of a typical lead core elastomeric bearing is shown in Figure 41.7. An associated hysteresis curve is shown in Figure 41.8. Typical bearing sizes and their load bearing capacities are given in Table 41.1 [7].

Lead core elastomeric isolation bearings are the most widely used isolation devices in bridge seismic design applications. They have been used in the seismic retrofit and new design in hundreds of bridges worldwide.

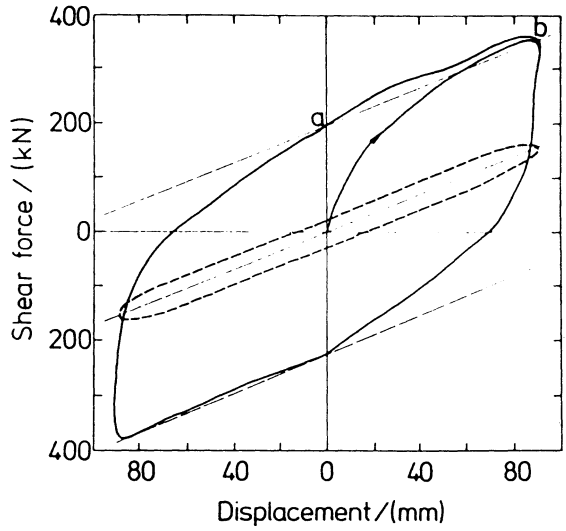


**FIGURE 41.8** Hysteresis loops of lead core rubber bearing.

### 41.3.2 Sliding Isolators

Sliding-type isolation bearings reduce the force transferred from superstructure to the supporting substructure when subject to earthquake excitations by allowing the superstructure to slide on a low friction surface usually made from stainless steel-PTFE. The maximum friction between the sliding surfaces limits the maximum force that can be transferred by the bearing. The friction between the surfaces will also dissipate energy. A major concern with relying only on simple sliding bearings for seismic application is the lack of centering force to restore the structure to its undisplaced position together with poor predictability and reliability of the response. This can be addressed by combining the slider with spring elements or, as in the case of friction pendulum isolation (FPI) bearings, by making the sliding surface curved such that the self-weight of the structure will help recenter the superstructure. In the following, the FPI bearings by Earthquake Protection Systems (EPS) will be presented as a representative of sliding-type isolation bearings.

The FPI bearing utilizes the characteristics of a simple pendulum to lengthen the natural period of an isolated structure. Typical construction of an FPI bearing is shown in Figure 41.9. It basically consists of a slider with strength-bearing spherical surface and a treated spherical concave sliding surface housed in a cast steel bearing housing. The concave surface and the surface of the slider have the same radius to allow a good fit and a relatively uniform pressure under vertical loads. The operation of the isolator is the same regardless of the direction of the concave surface. The size of the bearing is mainly controlled by the maximum design displacement.

The concept is really a simple one, as illustrated in Figure 41.10. When the superstructure moves relative to the supporting pier, it behaves like a simple pendulum. The radius, R, of the concave surface controls the isolator period,

$$T = 2\pi\sqrt{\frac{R}{g}} \tag{41.14}$$

where $g$ is the acceleration of gravity. The fact that the isolator period is independent of the mass of the supported structure is an advantage over the elastomeric isolators because fewer factors are involved in selecting an isolation bearing. For elastomeric bearings, in order to lengthen the period

**TABLE 41.1** Total Dead Plus Live-Load Capacity of Square DIS Bearings (kN)

| Plan Size | | Bonded Area | Rubber Layer Thickness, mm | | | |
|---|---|---|---|---|---|---|
| *W*(mm) | *B*(mm) | ($mm^2$) | 6.5 | 9.5 | 12.5 | 19 |
| 229 | 229 | 52,258 | 236 | 160 | 125 | 85 |
| 254 | 254 | 64,516 | 338 | 227 | 173 | 120 |
| 279 | 279 | 78,064 | 463 | 311 | 236 | 165 |
| 305 | 305 | 92,903 | 614 | 414 | 311 | 214 |
| 330 | 330 | 109,032 | 796 | 534 | 405 | 276 |
| 356 | 356 | 126,451 | 1,010 | 676 | 512 | 351 |
| 381 | 381 | 145,161 | 1,263 | 845 | 641 | 436 |
| 406 | 406 | 165,161 | 1,552 | 1,041 | 783 | 529 |
| 432 | 432 | 186,451 | 1,882 | 1,259 | 952 | 641 |
| 457 | 457 | 209,032 | 2,255 | 1,508 | 1,139 | 770 |
| 483 | 483 | 232,903 | 2,678 | 1,793 | 1,348 | 912 |
| 508 | 508 | 258,064 | 3,149 | 2,104 | 1,583 | 1,068 |
| 533 | 533 | 284,516 | 3,674 | 2,455 | 1,846 | 1,241 |
| 559 | 559 | 312,257 | 4,252 | 2,842 | 2,135 | 1,437 |
| 584 | 584 | 341,290 | 4,888 | 3,265 | 2,455 | 1,650 |
| 610 | 610 | 371,612 | 5,582 | 3,727 | 2,802 | 1,882 |
| 635 | 635 | 403,225 | 6,343 | 4,234 | 3,185 | 2,135 |
| 660 | 660 | 436,128 | 7,170 | 4,786 | 3,598 | 2,411 |
| 686 | 686 | 470,322 | 8,064 | 5,382 | 4,043 | 2,713 |
| 711 | 711 | 505,805 | 9,029 | 6,027 | 4,528 | 3,034 |
| 737 | 737 | 542,580 | 10,070 | 6,721 | 5,048 | 3,380 |
| 762 | 762 | 580,644 | 11,187 | 7,464 | 5,609 | 3,754 |
| 787 | 787 | 619,999 | 12,383 | 8,264 | 6,205 | 4,154 |
| 813 | 813 | 660,644 | 13,660 | 9,118 | 6,845 | 4,581 |
| 838 | 838 | 702,579 | 15,025 | 10,026 | 7,530 | 5,040 |
| 864 | 864 | 745,805 | 16,480 | 10,995 | 8,255 | 5,524 |
| 889 | 889 | 790,321 | 18,023 | 12,023 | 9,029 | 6,040 |
| 914 | 914 | 836,127 | 19,660 | 13,117 | 9,848 | 6,587 |

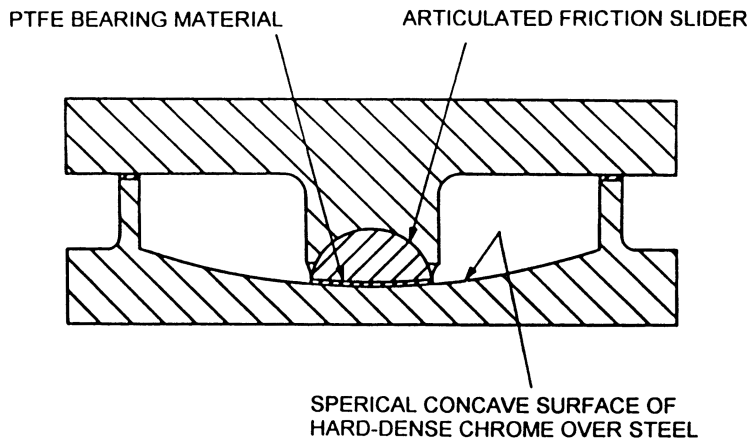


**FIGURE 41.9** Typical construction of a FPI.

of an isolator without varying the plan dimensions, one has to increase the height of the bearing which is limited by stability requirement. For FPI bearings, one can vary the period simply by changing the radius of the concave surface. Another advantage the FPI bearing has is high vertical load-bearing capacity, up to 30 million lb (130,000 kN) [10].

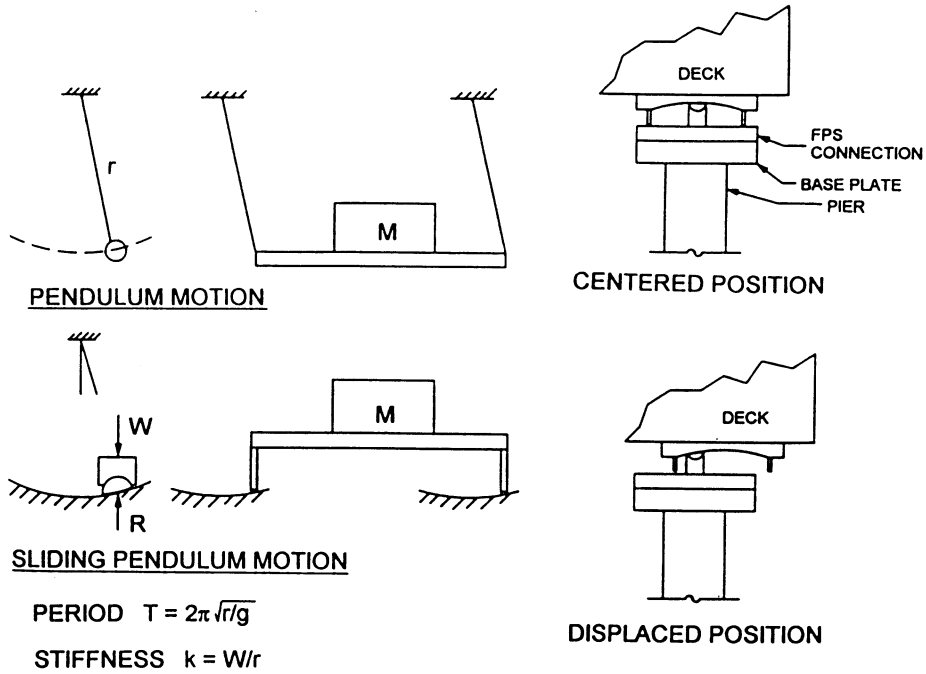


**FIGURE 41.10** Basic operating principle of FPI.

The FPI system behaves rigidly when the lateral load on the structure is less than the friction force, which can be designed to be less than nonseismic lateral loads. Once the lateral force exceeds this friction force, as is the case under earthquake excitation, it will respond at its isolated period. The dynamic friction coefficient can be varied in the range of 0.04 to 0.20 to allow for different levels of lateral resistance and energy dissipation.

The FPI bearings have been used in several building seismic retrofit projects, including the U.S. Court of Appeals Building in San Francisco and the San Francisco Airport International Terminal. The first bridge structure to be isolated by FPI bearings is the American River Bridge in Folsom, California. Figure 41.11 shows one of the installed bearings on top of the bridge pier. The maximum designed bearing displacement is 250 mm, and maximum vertical load is about 16,900 kN. The largest bearings have a plan dimension of 1150 × 1150 mm. The FPI bearings will also be used in the Benicia–Martinez Bridge in California when construction starts on the retrofit of this mile-long bridge. The bearings designed for this project will have a maximum plan dimension of 4500 × 4500 mm to accommodate a maximum designed displacement of 1200 mm [11].

### 41.3.3 Viscous Fluid Dampers

Viscous fluid dampers, also called hydraulic dampers in some of the literature, typically consist of a piston moving inside the damper housing cylinder filled with a compound of silicone or oil. Figure 41.12 shows typical construction of a Taylor Device's viscous fluid damper and its corresponding hysteresis curve. As the piston moves inside the damper housing, it displaces the fluid which in turn generates a resisting force that is proportional to the exponent of the velocity of the moving piston, i.e.,

$$F = cV^k \tag{41.15}$$

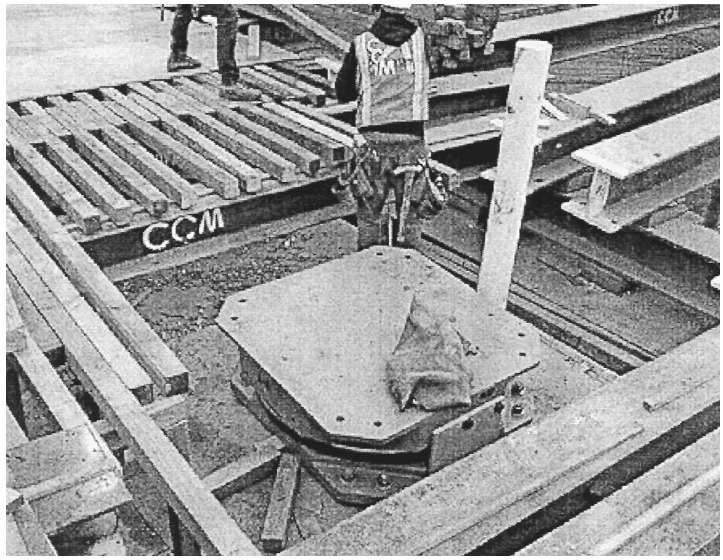


**FIGURE 41.11** A FPI bearing installed on a bridge pier.

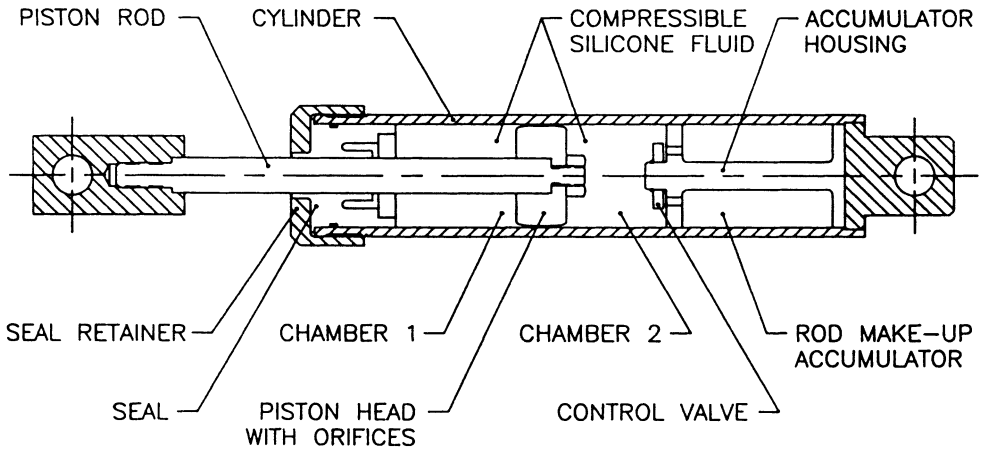


**FIGURE 41.12** Typical construction of a taylor devices fluid viscous damper.

where $c$ is the damping constant, $V$ is the velocity of the piston, and $k$ is a parameter that may be varied in the range of 0.1 to 1.2, as specified for a given application. If $k$ equals 1, we have a familiar linear viscous damping force. Again, the effectiveness of the damper can be represented by the amount of energy dissipated in one complete cycle of deformation:

$$E_d = \int F dx \tag{41.16}$$

The earlier applications of viscous fluid dampers were in the vibration isolation of aerospace and defense systems. In recent years, theoretical and experimental studies have been performed in an effort to apply the viscous dampers to structure seismic resistant design [4,12]. As a result, viscous

**TABLE 41.2** Fluid Viscous Damper Dimension Data (mm)

| Model | A | B | C | D | E | F |
|---|---|---|---|---|---|---|
| 100 kips (445 kN) | 3327 | 191 | 64 | 81 | 121 | 56 |
| 200 kips (990 kN) | 3353 | 229 | 70 | 99 | 127 | 61 |
| 300 kips (1335 kN) | 3505 | 292 | 76 | 108 | 133 | 69 |
| 600 kips (2670 kN) | 3937 | 406 | 152 | 191 | 254 | 122 |
| 1000 kips (4450 kN) | 4216 | 584 | 152 | 229 | 362 | 122 |
| 2000 kips (9900 kN) | 4572 | 660 | 203 | 279 | 432 | 152 |

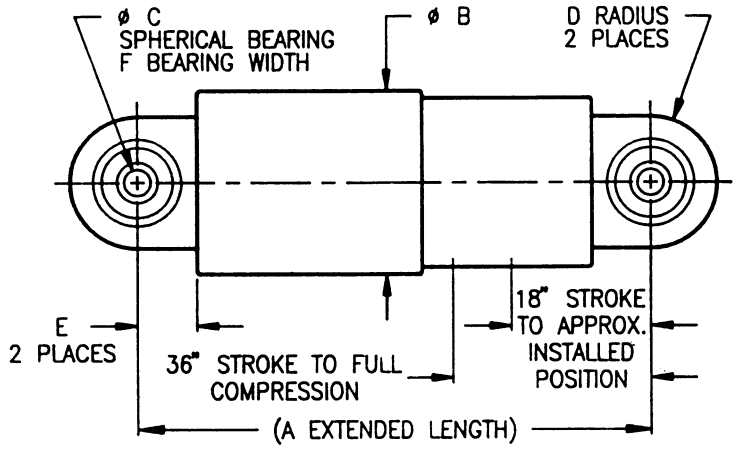


**FIGURE 41.13** Viscous damper dimension.

dampers have found applications in several seismic retrofit design projects. For example, they have been considered for the seismic upgrade of the Golden Gate Bridge in San Francisco [13], where viscous fluid dampers may be installed between the stiffening truss and the tower to reduce the displacement demands on wind-locks and expansion joints. The dampers are expected to reduce the impact between the stiffening truss and the tower. These dampers will be required to have a maximum stroke of about 1250 mm, and be able to sustain a peak velocity of 1880 mm/s. This requires a maximum force output of 2890 kN.

Fluid viscous dampers are specified by the amount of maximum damping force output as shown in Table 41.2 [14]. Also shown in Table 41.2 are dimension data for various size dampers that are typical for bridge applications. The reader is referred to Figure 41.13 for dimension designations.

### 41.3.4 Viscoelastic Dampers

A typical viscoelastic damper, as shown in Figure 41.14, consists of viscoelastic material layers bonded with steel plates. Viscoelastic material is the general name for those rubberlike polymer materials having a combined feature of elastic solid and viscous liquid when undergoing deformation. Figure 41.14 also shows a typical hysteresis curve of viscoelastic dampers. When the center plate moves relative to the two outer plates, the viscoelastic material layers undergo shear deformation. Under a sinusoidal cyclic loading, the stress in the viscoelastic material can be expressed as

$$\sigma = \gamma_0 \left(G' \sin \omega t + G'' \cos \omega t\right) \tag{41.17}$$

where $\gamma_0$ represents the maximum strain, $G'$ is shear storage modulus, and $G''$ is the shear loss modulus, which is the primary factor determining the energy dissipation capability of the viscoelastic material.

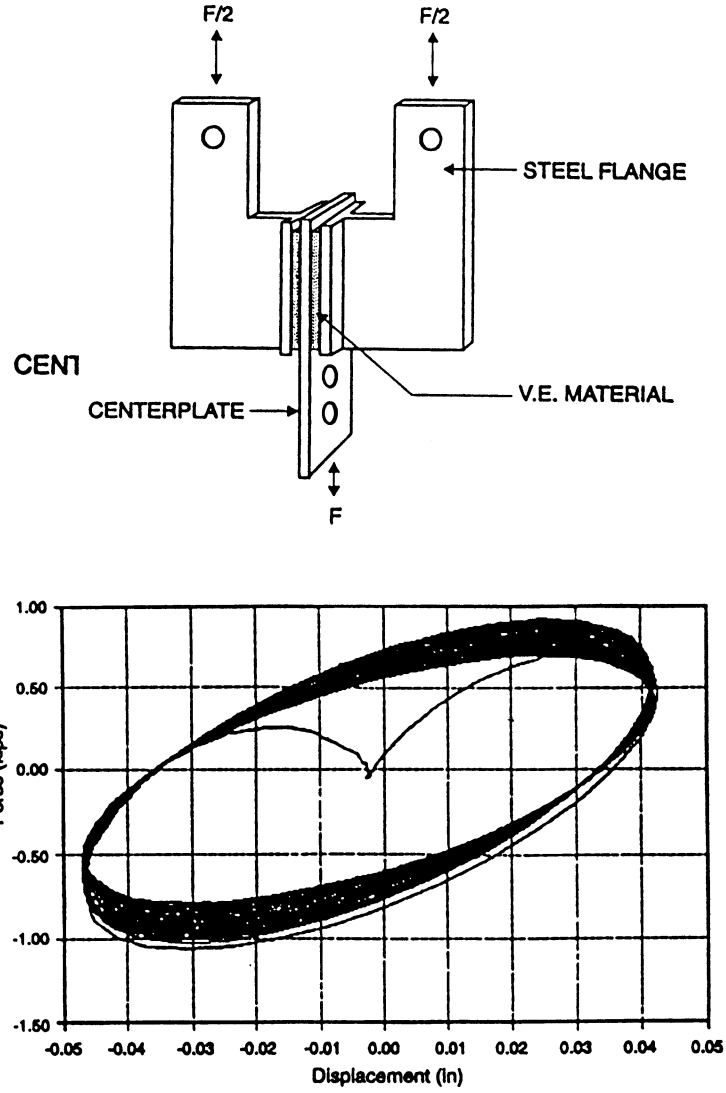


**FIGURE 41.14** Typical viscoelastic damper and its hysteresis loops.

After one complete cycle of cyclic deformation, the plot of strain vs. stress will look like the hysteresis shown in Figure 41.14. The area enclosed by the hysteresis loop represents the amount of energy dissipated in one cycle per unit volume of viscoelastic material:

$$e_d = \pi \gamma_0^2 G' \tag{41.18}$$

The total energy dissipated by viscoelastic material of volume $V$ can be expressed as

$$E_d = \pi \gamma_0^2 G'' V \tag{41.19}$$

The application of viscoelastic dampers to civil engineering structures started more than 20 years ago, in 1968, when more than 20,000 viscoelastic dampers made by the 3M Company were installed in the twin-frame structure of the World Trade Center in New York City to help resist wind load.

In the late 1980s, theoretical and experimental studies were first conducted for the possibility of applying viscoelastic dampers for seismic applications [9,15]. Viscoelastic dampers have since received increased attention from researchers and practicing engineers. Many experimental studies have been conducted on scaled and full-scale structural models. Recently, viscoelastic dampers were used in the seismic retrofit of several buildings, including the Santa Clara County Building in San Jose, California. In this case, viscoelastic dampers raised the equivalent damping ratio of the structure to 17% of critical [16].

### 41.3.5 Other Types of Damping Devices

There are several other types of damping devices that have been studied and applied to seismic resistant design with varying degrees of success. These include metallic yield dampers, friction dampers, and tuned mass dampers. Some of them are more suited for building applications and may be of limited effectiveness to bridge structures.

**Metallic Yield Damper.** Controlled use of sacrificial metallic energy dissipating devices is a relatively new concept [17]. A typical device consists of one or several metallic members, usually made of mild steel, which are subjected to axial, bending, or torsional deformation depending on the type of application. The choice between different types of metallic yield dampers usually depends on location, available space, connection with the structure, and force and displacement levels. One possible application of steel yield damper to bridge structures is to employ steel dampers in conjunction with isolation bearings. Tests have been conducted to combine a series of cantilever steel dampers with PTFE sliding isolation bearing.

**Friction Damper.** This type of damper utilizes the mechanism of solid friction that develops between sliding surfaces to dissipate energy. Several types of friction dampers have been developed for the purpose of improving seismic response of structures. For example, studies have shown that slip joints with friction pads placed in the braces of a building structure frame significantly reduced its seismic response. This type of braced friction dampers has been used in several buildings in Canada for improving seismic response [4,18].

**Tuned Mass Damper.** The basic principle behind tuned mass dampers (TMD) is the classic dynamic vibration absorber, which uses a relatively small mass attached to the main mass via a relatively small stiffness to reduce the vibration of the main mass. It can be shown that, if the period of vibration of the small mass is tuned to be the same as that of the disturbing harmonic force, the main mass can be kept stationary. In structural applications, a tuned mass damper may be installed on the top floor to reduce the response of a tall building to wind loads [4]. Seismic application of TMD is limited by the fact that it can only be effective in reducing vibration in one mode, usually the first mode.

## 41.4 Performance and Testing Requirements

Since seismic isolation and energy dissipation technologies are still relatively new and often the properties used in design can only be obtained from tests, the performance and test requirements are critical in effective applications of these devices. Testing and performance requirements, for the most part, are prescribed in project design criteria or construction specifications. Some nationally recognized design specifications, such as AASHO *Guide Specifications for Seismic Isolation Design* [19], also provide generic testing requirements.

Almost all of the testing specified for seismic isolators or energy dissipation devices require tests under static or simple cyclic loadings only. There are, however, concerns about how well will properties obtained from these simple loading tests correlate to behaviors under real earthquake

loadings. Therefore, a major earthquake simulation testing program is under way. Sponsored by the Federal Highway Administration and the California Department of Transportation, manufacturers of isolation and energy dissipation devices were invited to provide their prototype products for testing under earthquake loadings. It is hoped that this testing program will lead to uniform guidelines for prototype and verification testing as well as design guidelines and contract specifications for each of the different systems. The following is a brief discussion of some of the important testing and performance requirements for various systems.

### 41.4.1 Seismic Isolation Devices

For seismic isolation bearings, performance requirements typically specify the maximum allowable lateral displacements under seismic and nonseismic loadings, such as thermal and wind loads; horizontal deflection characteristics such as effective and maximum stiffnesses; energy dissipation capacity, or equivalent damping ratio; vertical deflections; stability under vertical loads; etc. For example, the AASHTO *Guide Specifications for Seismic Isolation Design* requires that the design and analysis of isolation system prescribed be based on prototype tests and a series of verification tests as briefly described in the following:

**Prototype Tests**:

I. Prototype tests need to be performed on two full-size specimens. These tests are required for each type and size similar to that used in the design.
II. For each cycle of tests, the force–deflection and hysteresis behavior of the specimen need to be recorded.
III. Under a vertical load similar to the typical average design dead load, the specimen need to be tested for
   A. Twenty cycles of lateral loads corresponding to the maximum nonseismic loads;
   B. Three cycles of lateral loading at displacements equaling 25, 50, 75, 100, and 125% of the total design displacement;
   C. Not less than 10 full cycles of loading at the total design displacement and a vertical load similar to dead load.
IV. The stability of the vertical load-carrying element need to be demonstrated by one full cycle of displacement equaling 1.5 times the total design displacement under dead load plus or minus vertical load due to seismic effect.

**System Characteristics Tests**:

I. The force–deflection characteristics need to be based on cyclic test results.
II. The effective stiffness of an isolator needs to be calculated for each cycle of loading as

$$k_{\text{eff}} = \frac{F_p - F_n}{\Delta_p - \Delta_n} \tag{41.20}$$

where $F_p$ and $F_n$ are the maximum positive and negative forces, respectively, and $\Delta_p$ and $\Delta_n$ are the maximum positive and negative displacements, respectively.

III. The equivalent viscous damping ratio $\xi$ of the isolation system needs to be calculated as

$$\xi = \frac{\text{Total Area}}{4\pi \sum \frac{kd^2}{2}} \tag{41.21}$$

where Total Area shall be taken as the sum of areas of the hysteresis loops of all isolators; the summation in the denominator represents the total strain energy in the isolation system.

In order for a specimen to be considered acceptable, the results of the tests should show positive incremental force-carrying capability, less than a specified amount of variation in effective stiffness between specimens and between testing cycles for any given specimen. The effective damping ratio also needs to be within certain range [19].

### 41.4.2 Testing of Energy Dissipation Devices

As for energy dissipation devices, there have not been any codified testing requirements published. The Federal Emergency Management Agency 1994 NEHRP Recommended Provisions for Seismic Regulation for New Buildings contains an appendix that addresses the use of energy dissipation systems and testing requirements [20]. There are also project-specific testing requirements and proposed testing standards by various damper manufacturers.

Generally speaking, testing is needed to obtain appropriate device parameters for design use. These parameters include the maximum force output, stroke distance, stiffness, and energy dissipation capability. In the case of viscous dampers, these are tested in terms of damping constant *C,* exponential constant, maximum damping force, etc. Most of the existing testing requirements are project specific. For example, the technical requirements for viscous dampers to be used in the retrofit of the Golden Gate Bridge specify a series of tests to be carried out on model dampers [13,21]. Prototype tests were considered to be impractical because of the limitation of available testing facilities. These tests include cyclic testing of model dampers to verify their constitutive law and longevity of seals and a drop test of model and prototype dampers to help relate cyclic testing to the behavior of the actual dampers. Because the tests will be on model dampers, some calculations will be required to extrapolate the behavior of the prototype dampers.

## 41.5 Design Guidelines and Design Examples

In the United States, design of seismic isolation for bridges is governed by the *Guide Specifications for Seismic Isolation Design* (hereafter known as "Guide Specifications") published by AASHTO in 1992. Specifications for the design of energy dissipation devices have not been systematically developed, while recommended guidelines do exist for building-type applications.

In this section, design procedure for seismic isolation design and a design example will be presented mainly based on the AASHTO Guide Specifications. As for the design of supplemental energy dissipation, an attempt will be made to summarize some of the guidelines for building-type structures and their applicability to bridge applications.

### 41.5.1 Seismic Isolation Design Specifications and Examples

The AASHTO Guide Specifications were written as a supplement to the AASHTO *Standard Specifications for the Seismic Design of Highway Bridges* [22] (hereafter known as "Standard Specifications"). Therefore, the seismic performance categories and site coefficients are identical to those specified in the Standard Specifications. The response modification factors are the same as in the Standard Specifications except that a reduced *R* factor of 1.5 is permitted for essentially elastic design when the design intent of seismic isolation is to eliminate or significantly reduce damage to the substructure.

#### General Requirements

There are two interrelated parts in designing seismic isolation devices for bridge applications. First of all, isolation bearings must be designed for all nonseismic loads just like any other bearing devices. For example, for lead core rubber isolation bearings, both the minimum plan size and the thickness of individual rubber layers are determined by the vertical load requirement. The minimum isolator

**TABLE 41.3** Damping Coefficient B

| Damping Ratio (ξ) | ≤ 2% | 5% | 10% | 20% | 30% |
|---|---|---|---|---|---|
| B | 0.8 | 1.0 | 1.2 | 1.5 | 1.7 |

*Source*: AASHTO, *Guide Specification for Seismic Isolation Design*, Washington, D.C., 1991. With permission.

height is controlled by twice the displacement due to combined nonseismic loads. The minimum diameter of the lead core is determined by the requirement to maintain elastic response under combined wind, brake, and centrifugal forces. Similar requirements can also be applied to other types of isolators. In addition to the above requirements, the second part of seismic isolation design is to satisfy seismic safety requirements. The bearing must be able to support safely the vertical loads at seismic displacement. This second part is accomplished through the analysis and design procedures described below.

## Methods of Analysis

The Guide Specifications allow treatment of energy dissipation in isolators as equivalent viscous damping and stiffness of isolated systems as effective linear stiffness. This permits both the single and multimodal methods of analysis to be used for seismic isolation design. Exceptions to this are isolated systems with damping ratios greater than 30% and sliding type of isolators without a self-centering mechanism. Nonlinear time history analysis is required for these cases.

Single-Mode Spectral Analysis

In this procedure, equivalent static force is given by the product of the elastic seismic force coefficient $C_s$ and dead load $W$ of the superstructure supported by isolation bearings, i.e.,

$$F = C_s W \tag{41.22}$$

$$C_s = \frac{\sum k_{\text{eff}} \times d_i}{W} \tag{41.23}$$

$$C_s = \frac{AS_i}{T_e B} \tag{41.24}$$

where

$\sum k_{\text{eff}}$ = the sum of the effective linear stiffness of all bearings supporting the superstructure

$d_i = \dfrac{10AS_iT_e}{B}$ = displacement across the isolation bearings

$A$ = the acceleration coefficient

B = the damping coefficient given in Table 41.3

$T_e = \sqrt{\dfrac{W}{g\sum k_{\text{eff}}}}$ = the period of vibration

The equivalent static force must be applied independently to the two orthogonal axes and combined per the procedure of the standard specifications. The effective linear stiffness should be calculated at the design displacement.

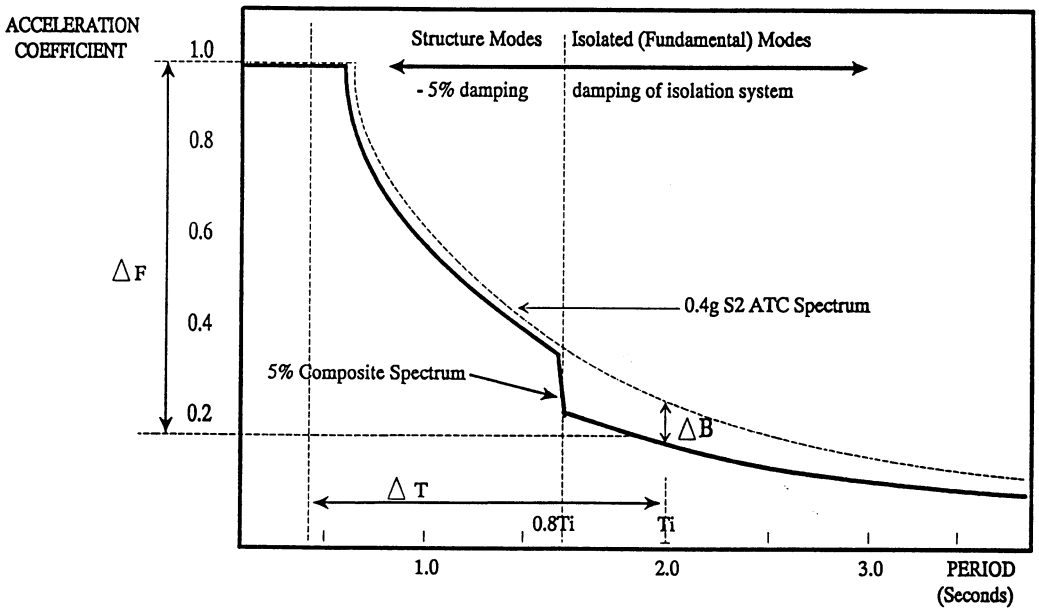


**FIGURE 41.15** Modified input response spectrum.

Response Spectrum Analysis
This procedure is the same as specified in the Standard Specifications using the 5% damping ground motion response spectra with the following modifications:

1. The isolation bearings are represented by their effective stiffness values.
2. The response spectrum is modified to include the effect of higher damping of the isolated system. This results in a reduction of the response spectra values for the isolated modes. For all the other modes, the 5% damping response spectra should be used.

A typical modified response spectrum is shown in Figure 41.15.

Time History Analysis
As mentioned earlier, time history analysis is required for isolation systems with high damping ratio (>30%) or non-self-centering isolation systems. The isolation systems need to be modeled using nonlinear force–deflection characteristics of the isolator obtained from tests. Pairs of ground acceleration time history recorded from different events should be selected. These acceleration time histories should be frequency-scaled to match closely the appropriate response spectra for the site. Recommended methods for scaling are also given in the Guide Specifications. At least three pairs of time histories are required by the code. Each pair should be simultaneously applied to the model. The maximum response should be used for the design.

## Design Displacement and Design Force

It is necessary to know and limit the maximum displacement of an isolation system resulting from seismic loads and nonseismic service loads for providing adequate clearance and design structural elements. The Guide Specifications require that the total design displacement be the greater of 50% of the elastomer shear strain in an elastomeric bearing system and the maximum displacement resulted from the combination of loads specified in the Standard Specifications.

Design forces for a seismically isolated bridge are obtained using the same load combinations as given for a conventionally designed bridge. Connection between superstructure and substructure shall be designed using force $F = k_{\text{eff}} d_i$. Columns and piers should be designed for the maximum

force that may be developed in the isolators. The foundation design force needs not to exceed the elastic force nor the force resulted from plastic hinging of the column.

### Other Requirements

It is important for an isolation system to provide adequate rigidity to resist frequently occurring wind, thermal, and braking loads. The appropriate allowed lateral displacement under nonseismic loads is left for the design engineer to decide. On the lateral restoring force, the Guide Specifications require a restoring force that is 0.25W greater than the lateral force at 50% of the design displacement. For systems not configured to provide a restoring force, more stringent vertical stability requirements have to be met.

The Guide Specifications recognize the importance of vertical stability of an isolated system by requiring a factor of safety not less than three for vertical loads in its undeformed state. A system should also be stable under the dead load plus or minus the vertical load due to seismic load at a horizontal displacement of 1.5 times the total design displacement. For systems without a lateral restoring force, this requirement is increased to three times the total design displacement.

### Guidelines for Choosing Seismic Isolation

What the Guide Specifications do not cover are the conditions under which the application of seismic isolation becomes necessary or most effective. Still, some general guidelines can be drawn from various literatures and experiences as summarized below.

One factor that favors the use of seismic isolation is the level of acceptable damage to the bridge. Bridges at critical strategic locations need to stay open to traffic following a seismic event with no damage or minor damages that can be quickly repaired. This means that the bridges are to be essentially designed elastically. The substructure pier and foundation cost could become prohibitive if using conventional design. The use of seismic isolation may be an economic solution for these bridges, if not the only solution. This may apply to both new bridge design and seismic upgrade of existing bridges.

Sometimes, it is desirable to reduce the force transferred to the superstructure, as in the case of seismic retrofit design of the Benicia–Martinez Bridge, in the San Francisco Bay, where isolation bearings were used to limit the forces in the superstructure truss members [11].

Another factor to consider is the site topography of the bridge. Irregular terrain may result in highly irregular structure configurations with significant pier height differences. This will result in uneven seismic force distributions among the piers and hence concentrated ductility demands. Use of seismic isolation bearings will make the effective stiffness and expected displacement of piers closer to each other resulting in a more even force distribution [23].

For seismic upgrading of existing bridges, isolation bearings can be an effective solution for understrength piers, insufficient girder support length, and inadequate bearings.

In some cases, there may not be an immediate saving from the use of seismic isolation over a conventional design. Considerations need to be given to a life-cycle cost comparison because the use of isolation bearings generally means much less damages, and hence lower repair costs in the long run.

### Seismic Isolation Design Example

As an example, a three-span continuous concrete box-girder bridge structure, shown in Figure 41.16, will be used here to demonstrate the seismic isolation design procedure. Material and structure properties are also given in Figure 41.16. The bridge is assumed to be in a high seismic area with an acceleration coefficient $A$ of 0.40, soil profile Type II, S = 1.2. For simplicity, let us use the single mode spectral analysis method for the analysis of this bridge. Assuming that the isolation bearings will be designed to provide an equivalent viscous damping of 20%, with a damping coefficient, $B$, of 1.5. The geometry and section properties of the bridge are taken from the worked example in the Standard Specifications with some modifications.

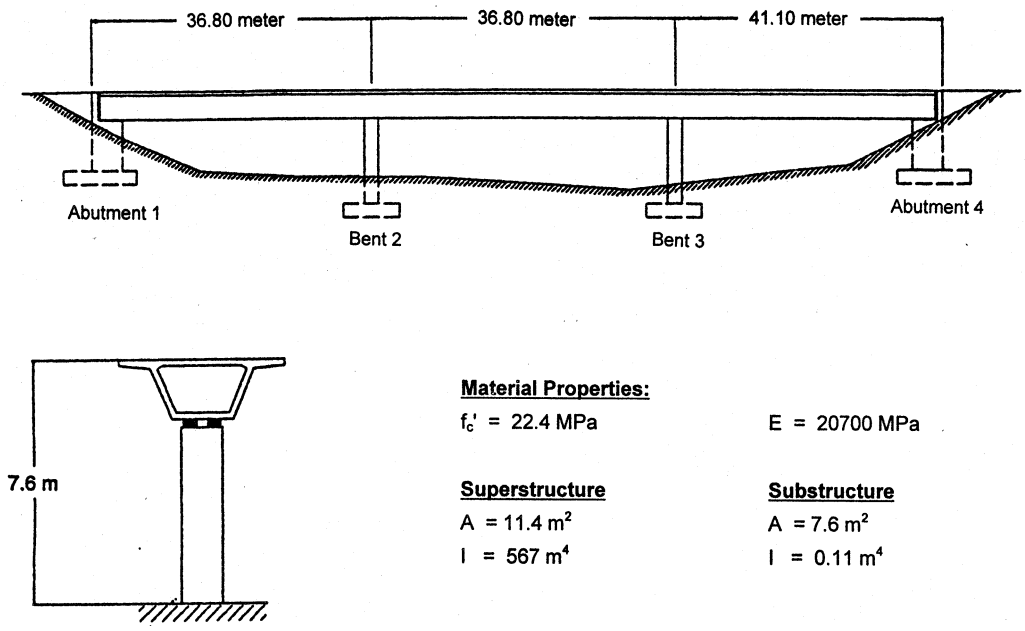


**FIGURE 41.16** Example three-span bridge structure.

Force Analysis

Maximum tributary mass occurs at Bent 3, with a mass of 123 ft$^2$ × 150 lb/ft$^3$ × 127.7 ft = 2356 kips (1,065,672 kg). Consider earthquake loading in the longitudinal direction. For fixed top of column support, the stiffness $k_0 = (12\ EI)/H^3 = 12 \times 432{,}000 \times 39/25^3 = 12{,}940$ kips/ft (189 kN/mm). This results in a fixed support period

$$T_0 = 2\pi\sqrt{\frac{W}{k_0 g}} = 2\pi\sqrt{\frac{2356}{12940 \times 32.3}} = 0.47\text{s}$$

The corresponding elastic seismic force

$$F_0 = C_s W = \frac{1.2AS}{T^{2/3}} = \frac{1.2 \times 0.4 \times 1.2}{0.47^{2/3}} W = 0.95W = 2238\ \text{kip}\ \ (9955\ \text{kN})$$

Now, let us assume that, with the introduction of seismic isolation bearings at the top of the columns, the natural period of the structure becomes 2.0 s, and damping $B = 1.5$. From Eqs. (41.22) and (41.24), the elastic seismic force for the isolated system,

$$F_i = C_s W = \frac{AS_i}{T_e B} W = \frac{0.4 \times 1.2}{2.0 \times 1.5} W = 0.16W = 377\ \text{kips}\ \ (1677\ \text{kN})$$

Displacement across the isolation bearing

$$d = \frac{10AS_i T_e}{B} = \frac{10 \times 0.4 \times 1.2 \times 2.0}{1.5} = 6.4\ \text{in.}\ (163\ \text{mm})$$

**TABLE 41.4** Seismic Isolation Design Example Results

| | | | | | | | |
|---|---|---|---|---|---|---|---|
| $T_e$ | (s) | 0.5 | 1.0 | 1.5 | 2.0 | 2.5 | 3.0 |
| $k_{\text{eff}}$ | (kips/in) | 306.48 | 76.62 | 34.05 | 19.16 | 12.26 | 8.51 |
| | (kN/mm) | (53.67) | (13.42) | (5.96) | (3.35) | (2.15) | (1.49) |
| $d$ | (in.) | 1.60 | 3.20 | 4.80 | 6.40 | 8.00 | 9.60 |
| | (mm) | (40.64) | (81.28) | (121.92) | (162.56) | (203.20) | (243.84) |
| $C_s$ | | 0.64 | 0.32 | 0.21 | 0.16 | 0.13 | 0.11 |
| $F_i$ | (kip) | 1507.84 | 753.92 | 502.61 | 376.96 | 301.57 | 251.31 |
| | (kN) | (6706.87) | (3353.44) | (2235.62) | (1676.72) | (1341.37) | (1117.81) |

Table 41.4 examines the effect of isolation period on the elastic seismic force. For an isolated period of 0.5 s, which is approximately the same as the fixed support structure, the 30% reduction in elastic seismic force represents basically the effect of the added damping of the isolation system.

Isolation Bearing Design

Assume that four elastomeric (lead core rubber) bearings are used at each bent for this structure. Vertical local due to gravity load is $P = 2356/4 = 589$ kips (2620 kN). We will design the bearings such that the isolated system will have a period of 2.5 s.

$$T_e = \sqrt{\frac{W}{g\sum k_{\text{eff}}}}$$

and

$$k_{\text{eff}} = 4\left(\frac{GA}{T}\right)$$

where $T$ is the total thickness of the elastomer. We have

$$\frac{GA}{T} = 3.06 \text{ kip/in. } (0.54 \text{ kN/mm})$$

Assuming a shear modulus $G = 145$ psi (1.0 MPa) and bearing thickness of $T = 18$ in. (457 mm) with thickness of each layer $t_i$ equaling 0.5 in . This gives a bearing area $A = 380$ in$^2$ (245,070 mm$^2$). Hence, a plan dimension of 19.5 × 19.5 in. (495 × 495 mm).

Check shape factor:

$$S = \frac{ab}{2t_i(a+b)} = \frac{19.5\times19.5}{2\times0.5(19.5+19.5)} \quad \text{OK}$$

Shear strain in the elastomer is the critical characteristic for the design of elastomeric bearings.

Three shear strain components make up the total shear strain; these are shear strains due to vertical compression, rotation, and horizontal shear deformation. In the Guide Specifications, the shear strain due to compression by vertical load is given by

$$\gamma_c = \frac{3SW}{2A_rG(1+2kS^2)}$$

where $A_r = 19.5 \times (19.5 \text{ in.} - 8.0 \text{ in.}) = 224.3 \text{ in.}^2$ is the reduced bearing area representing the effective bearing area when undergoing horizontal displacement. In this case horizontal displacement is 8.0 in. For the purpose of presenting a simple example, an approximation of the previous expression can be used:

$$\gamma_c = \frac{\sigma}{GS} = \frac{589 \times 1000}{224.3 \times 145 \times 9.75} = 1.85$$

Shear strain due to horizontal shear deformation

$$\gamma_s = \frac{d}{T} = \frac{8 \text{ in.}}{18 \text{ in.}} = 0.44$$

and shear strain due to rotation

$$\gamma_r = \frac{B^2\theta}{2t_i T} = \frac{19.5^2 \times 0.01}{2 \times 0.5 \times 18} = 0.21$$

The Guide Specifications require that the sum of all three shear strain components be less than 50% of the ultimate shear strain of the elatomer, or 5.0, whichever is smaller. In this example, the sum of all three shear strain components equals $2.50 < 5.0$.

In summary, we have designed four elastomeric bearings at each bent with a plan dimension of 19.5 × 19.5 in. (495 × 495 mm) and 36 layers of 0.5 in. elastomer with $G = 145$ psi (1 MPa).

## 41.5.2 Guidelines for Energy Dissipation Devices Design

There are no published design guidelines or specifications for application of damping devices to bridge structures. Several recommended guidelines for application of dampers to building structures have been in development over the last few years [20,24,25]. It is hoped that a brief summary of these developments will be beneficial to bridge engineers.

### General Requirements

The primary function of an energy dissipation device in a structure is to dissipate earthquake-induced energy. No special protection against structural or nonstructural damage is sought or implied by the use of energy dissipation systems.

Passive energy dissipation systems are classified as displacement-dependent, velocity-dependent, or other. The fluid damper and viscoelastic damper as discussed in Section 41.3 are examples of the velocity-dependent energy dissipation system. Friction dampers are displacement-dependent. Different models need to be used for different classes of energy dissipation systems. In addition to increasing the energy dissipation capacity of a structure, energy dissipation systems may also alter the structure stiffness. Both damping and stiffness effects need to be considered in designing energy dissipation systems.

### Analysis Procedures

The use of linear analysis procedures is limited to viscous and viscoelastic energy dissipation systems. If nonlinear response is likely or hysteretic or other energy dissipaters are to be analyzed and designed, nonlinear analysis procedure must be followed. We will limit our discussion to linear analysis procedure.

Similar to the analysis of seismic isolation systems, linear analysis procedures include three methods: linear static, linear response spectrum, and linear time history analysis.

When using the linear static analysis method, one needs to make sure that the structure, exclusive of the dampers, remains elastic, that the combined structure damper system is regular, and that effective damping does not exceed 30%. The earthquake-induced displacements are reduced due to equivalent viscous damping provided by energy dissipation devices. This results in reduced base shears in the building structure.

The acceptability of the damped structure system should be demonstrated by calculations such that the sum of gravity and seismic loads at each section in each member is less than the member or component capacity.

The linear dynamic response spectrum procedure is used for more complex structure systems, where structures are modeled as MDOF systems. Modal response quantities are reduced based on the amount of equivalent modal damping provided by supplemental damping devices.

#### Detailed System Requirements

Other factors that need to be considered in designing supplemental damping devices for seismic applications are environmental conditions, nonseismic lateral loads, maintenance and inspection, and manufacturing quality control.

Energy dissipation devices need to be designed with consideration given to environmental conditions including aging effect, creep, and ambient temperature. Structures incorporated with energy-dissipating devices that are susceptible to failure due to low-cycle fatigue should resist the prescribed design wind forces in the elastic range to avoid premature failure. Unlike conventional construction materials that are inspected on an infrequent basis, some energy dissipation hardware will require regular inspections. It is, therefore, important to make these devices easily accessible for routine inspection and testing or even replacement.

## 41.6 Recent Developments and Applications

The last few years have seen significantly increased interest in the application of seismic isolation and supplemental damping devices. Many design and application experiences have been published. A shift from safety-only-based seismic design philosophy to a safety-and-performance-based philosophy has put more emphasis on limiting structural damage by controlling structural seismic response. Therefore, seismic isolation and energy dissipation have become more and more attractive alternatives to traditional design methods. Design standards are getting updated with the new development both in theory and technology. While the Guide Specifications referenced in this chapter addresses mainly elastomeric isolation bearing, new design specifications under development and review will include provisions for more types of isolation devices [26].

### 41.6.1 Practical Applications of Seismic Isolation

Table 41.5 lists bridges in North America that have isolation bearings installed. This list, as long as it looks, is still not complete. By some estimates, there have been several hundred isolated bridges worldwide and the number is growing. The Earthquake Engineering Research Center (EERC) at the University of California, Berkeley keeps a complete listing of the bridges with isolation and energy dissipation devices. Table 41.5 is based on information available from the EERC Internet Web site.

### 41.6.2 Applications of Energy Dissipation Devices to Bridges

Compared with seismic isolation devices, the application of energy dissipation devices as an independent performance improvement measure is lagging behind. This is due, in part, to the lack of code development and limited applicability of the energy dissipation devices to bridge-type structures as discussed earlier. Table 41.6 gives a list of bridge structures with supplemental damping devices against seismic and wind loads. This table is, again, based on information available from the EERC Internet Web site.

**TABLE 41.5** Seismically-Isolated Bridges in North America

| Bridge | Location | | Owner | Engineer | Bridge Description | Bearing Type | Design Criteria |
|---|---|---|---|---|---|---|---|
| Dog River Bridge, New, 1992 | AL | Mobile Co. | Alabama Hwy = 2E Dept. | Alabama Hwy. Dept. | Three-span cont. steel plate girders | LRB (DIS/Furon) | AASHTO Category A |
| Deas Slough Bridge, Retrofit, 1990 | BC | Richmond (Hwy. 99 over Deas Slough), | British Columbia Ministry of Trans. & Hwys. | PBK Eng. Ltd. | Three-span cont. riveted haunched steel plate girders | LRB (DIS/Furon) | AASHTO $A = 0.2g$, Soil profile, Type III |
| Burrard Bridge Main Spans, Retrofit, 1993 | BC | Vancouver (Burrard St. over False Cr.), | City of Vancouver | Buckland & Taylor Ltd. | Side spans are simple span deck trusses; center span is a Pratt through truss | LRB (DIS/Furon) | AASHTO $A = 0.21g$, Soil profile, Type I |
| Queensborough Bridge, Retrofit, 1994 | BC | New Westminster (over N. arm of Fraser River), | British Columbia Ministry of Trans. & Hwys. | Sandwell Eng. | High-level bridge, three-span cont. haunched steel plate girders; two-girder system with floor beams | LRB (DIS/Furon) | AASHTO $A = 0.2g$, Soil profile, Type I |
| Roberts Park Overhead, New, 1996 | BC | Vancouver (Deltaport Extension over BC Rail tracks) | Vancouver Port Corp. | Buckland & Taylor Ltd. | Five-span continuous curved steel plate girders, three girder lines | LRB | AASHTO $A = 0.26g$, Soil profile, Type II |
| Granville Bridge, Retrofit, 1996 | BC | Vancouver, Canada | — | — | — | FIP | — |
| White River Bridge, 1997 (est.) | YU | Yukon, Canada | Yukon Trans. Services | — | — | FPS | — |
| Sierra Pt. Overhead, Retrofit, 1985 | CA | S. San Francisco (U.S. 101 over S.P. Railroad) | Caltrans | Caltrans | Longitudinal steel plate girders, trans. steel plate bent cap girders | LRB (DIS/Furon) | Caltrans $A = 0.6g$, 0 to 10 ft alluvium |
| Santa Ana River Bridge, Retrofit, 1986 | CA | Riverside | MWDSC | Lindvall, Richter & Assoc. | Three 180 ft simple span through trusses, 10 steel girder approach spans | LRB (DIS/Furon) | ATC A = 0.4*g*, Soil profile, Type II |
| Eel River Bridge, Retrofit, 1987 | CA | Rio Dell (U.S. 101 over Eel River) | Caltrans | Caltrans | Two 300 ft steel through truss simple spans | LRB (DIS/Furon) | Caltrans $A = 0.5g$, < 150 ft alluvium |
| Main Yard Vehicle Access Bridge, Retrofit, 1987 | CA | Long Beach (former RR bridge over Long Beach Freeway) | LACMTA | W. Koo & Assoc., Inc. | Two 128 ft simple span steel through plate girders, steel floor beams, conc. deck | LRB (DIS/Furon) | Caltrans $A = 0.5g$, 10 to 80 ft alluvium |
| All-American Canal Bridge, Retrofit, 1988 | CA | Winterhaven, Imperial Co. (I-8 over All-American Canal) | Caltrans | Caltrans | Cont. steel plate girders (replacing former steel deck trusses) | LRB (DIS/Furon) | Caltrans $A = 0.6g$, >150 ft alluvium |
| Carlson Boulevard Bridge, New, 1992 | CA | Richmond (part of 23rd St. Grade Separation Project) | City of Richmond | A-N West, Inc. | Simple span multicell conc. box girder | LRB (DIS/Furon) | Caltrans $A = 0.7g$, 80 to 150 ft alluvium |
| Olympic Boulevard Separation, New, 1993 | CA | Walnut Creek (part of the 24/680 Reconstruction Project) | Caltrans | Caltrans | Four-span cont. steel plate girders | LRB (DIS/Furon) | Caltrans $A = 0.6g$, 10 to 80 ft alluvium |

| | | | | | | | |
|---|---|---|---|---|---|---|---|
| Alemany Interchange, Retrofit, 1994 | CA | I-280/U.S. 101 Interchange, San Francisco | Caltrans | PBQD | Single and double deck viaduct, R.C. box girders and cols., 7-cont. units | LRB (DIS/Furon) | Caltrans $A = 0.5g$, 10 to 80 ft alluvium |
| Route 242/I-680 Separation, Retrofit, 1994 | CA | Concord (Rte. 242 SB over I-680) | Caltrans | HDR Eng., Inc. | 8 ft-deep cont. prestressed conc. box girder | LRB (DIS/Furon) | Caltrans $A = 0.53g$, 80 to 150 ft alluvium |
| Bayshore Boulevard Overcrossing, Retrofit, 1994 | CA | San Francisco (Bayshore Blvd. over U.S. 101) | Caltrans | Winzler and Kelly | Continuous welded steel plate girders | LRB (DIS/Furon) | Caltrans $A = 0.53g$, 0 to 10 ft alluvium |
| 1st Street over Figuero, Retrofit, 1995 | CA | Los Angeles | City of Los Angeles | Kercheval Engineers | Continuous steel plate girders with tapered end spans | LRB | Caltrans $A = 0.6g$, 0 to 10 ft alluvium |
| Colfax Avenue over L.A. River, Retrofit, 1995 | CA | Los Angeles | City of Los Angeles | Kercheval Engineers | Deck truss center span flanked by short steel beam spans | LRB (DIS) | Caltrans $A = 0.5g$, 10 to 80 ft alluvium |
| Colfax Avenue over L.A. River, Retrofit, 1995 | CA | Los Angeles | City of Los Angeles | — | — | Eradiquake (RJ Watson) | — |
| 3-Mile Slough, Retrofit, 1997 (est.) | CA | — | Caltrans | — | — | LRB (Skellerup) | — |
| Rio Vista, Retrofit, 1997 (est.) | CA | — | Caltrans | — | — | LRB (Skellerup) | — |
| Rio Mondo Bridge, Retrofit, 1997 (est.) | CA | — | Caltrans | — | — | FPS (EPS) | — |
| American River Bridge City of Folsom, New, 1997 (est.) | CA | Folsom | City of Folsom | -HDR | Ten-span, 2-frame continuous concrete box girder bridge | FPS (EPS) | Caltrans $A = 0.5$g, 10 to 80 ft alluvium |
| GGB North Viaduct, Retrofit, 1998 (est.) | CA | — | GGBHTD | — | — | LRB | — |
| Benicia–Martinez Bridge Retrofit, 1998 (est.) | CA | — | Caltrans | — | — | FPS (EPS) | — |
| Coronado Bridge, Retrofit, 1998 (est.) | CA | — | Caltrans | — | — | HDR (not selected) | — |
| Saugatuck River Bridge, Retrofit, 1994 | CT | Westport (I-95 over Saugatuck R.) | ConnDOT | H.W. Lochner, Inc. | Three cont. steel plate girder units of 3, 4, and 3 spans | LRB (DIS/Furon) | AASHTO $A = 0.16g$, Soil profile, Type II |
| Lake Saltonstall Bridge, New, 1995 | CT | E. Haven & Branford (I-95 over Lake Saltonstall) | ConnDOT | Steinman Boynton Gronquist & Birdsall | Seven-span cont. steel plate girders | LRB (DIS/Furon) | AASHTO $A = 0.15g$, Soil profile, Type III |
| RT 15 Viaduct, 1996 | CT | Hamden | ConnDOT | Boswell Engineers | — | EradiQuake (RJ Watson) | — |
| Sexton Creek Bridge, New, 1990 | IL | Alexander Co. (IL Rte. 3 over Sexton Creek) | ILDOT | ILDOT | Three-span cont. steel plate girders | LRB (DIS/Furon) | AASHTO $A = 0.2g$, Soil profile, Type III |

**TABLE 41.5 (continued)** Seismically-Isolated Bridges in North America

| Bridge | Location | | Owner | Engineer | Bridge Description | Bearing Type | Design Criteria |
|---|---|---|---|---|---|---|---|
| Cache River Bridge, Retrofit, 1991 | IL | Alexander Co. (IL Rte. 3 over Cache R. Diversion Channel) | ILDOT | ILDOT | Three-span cont. steel plate girders | LRB (DIS/Furon) | AASHTO $A = 0.2g$, Soil profile, Type III |
| Route 161 Bridge, New, 1991 | IL | St. Clair Co. | ILDOT | Hurst-Rosche Engrs., Inc. | Four-span cont. steel plate girders | LRB (DIS/Furon) | AASHTO $A = 0.14g$, Soil profile, Type III |
| Poplar Street East Approach, Bridge #082-0005, Retrofit, 1992 | IL | E. St. Louis (carrying I-55/70/64 across Mississippi R.) | ILDOT | Sverdrup Corp. & Hsiong Assoc. | Two dual steel plate girder units supported on multicol. or wall piers; piled foundations | LRB (DIS/Furon) | AASHTO $A = 0.12g$, Soil profile, Type III |
| Chain-of-Rocks Road over FAP 310, New, 1994 | IL | Madison Co. | ILDOT | Oates Assoc. | Four-span cont. curved steel plate girders | LRB (DIS/Furon) | AASHTO $A = 0.13g$, Soil profile, Type III |
| Poplar Street East Approach, Roadway B, New, 1994 | IL | E. St. Louis | ILDOT | Sverdrup Corp. | Three-, four- and five-span cont. curved steel plate girder units | LRB (DIS/Furon) | AASHTO $A = 0.12g$, Soil profile, Type III |
| Poplar Street East Approach, Roadway C, New, 1995 | IL | E. St. Louis | ILDOT | Sverdrup Corp. | Three-, four- and five-span cont. curved steel plate girder units | LRB (DIS/Furon) | AASHTO $A = 0.12g$, Soil profile, Type III |
| Poplar Street Bridge, Retrofit, 1995 | IL | — | ILDOT | — | — | — | — |
| RT 13 Bridge, 1996 | IL | Near Freeburg | ILDOT | Casler, Houser & Hutchison | — | EradiQuake (RJ Watson) | — |
| Wabash River Bridge, New, 1991 | IN | Terra Haute, Vigo Co. (U.S.-40 over Wabash R = 2E) | INDOT | Gannett Flemming | Seven-span cont. steel girders | LRB (DIS/Furon) | AASHTO $A = 0.1g$, Soil profile, Type II |
| US-51 over Minor Slough, New, 1992 | KY | Ballard Co. | KTC | KTC | Three 121 ft simple span prestressed conc. I girders with cont. deck | LRB (DIS/Furon) | AASHTO $A = 0.25g$, Soil profile, Type II |
| Clays Ferry Bridge, Retrofit, 1995 | KY | I-75 over Kentucky R. | KTC | KTC | Five-span cont. deck truss, haunched at center two piers | LRB (DIS/Furon) | AASHTO $A = 0 = 2E1g$, Soil profile, Type I |
| Main Street Bridge, Retrofit, 1993 | MA | Saugus (Main St. over U.S. Rte 1) | MHD | Vanasse Hangen Brustlin, Inc. | Two-span cont. steel beams with conc. deck | LRB (DIS/Furon) | AASHTO $A = 0.17g$, Soil profile, Type I |
| Neponset River Bridge, New, 1994 | MA | New Old Colony RR over Neponset R. between Boston and Quincy | MBTA | Sverdrup Corp. | Simple span steel through girders; double-track ballasted deck | LRB (DIS/Furon) | AASHTO $A = 0.15g$, Soil profile, Type III |

| | | | | | | | |
|---|---|---|---|---|---|---|---|
| South Boston Bypass Viaduct, New, 1994 | MA | S. Boston | MHDCATP | DRC Consult., Inc. | Conc. deck supported with three trapez. steel box girders; 10-span cont. unit with two curved trapez. steel box girders | LRB (DIS/Furon) | AASHTO $A = 0.17g$, Soil profile, Type III |
| South Station Connector, New, 1994 | MA | Boston | MBTA | HNTB | Curved, trapezoidal steel ox girders. | LRB (DIS) | AASHTO $A = 0.18g$, Soil profile, Type III |
| North Street Bridge No. K-26, Retrofit, 1995 | MA | Grafton (North Street over Turnpike) | MTA | The Maguire Group Inc. | Steel beams, two-span continuous center unit flanked by simple spans. | LRB (DIS) | AASHTO $A = 0.17g$, Soil profile, Type II |
| Old Westborough Road Bridge, Retrofit, 1995 | MA | Grafton | MTA | The Maguire Group Inc. | Steel beams, two-span continuous center unit flanked by simple spans. | LRB (DIS) | AASHTO $A = 0.17g$, Soil profile, Type I |
| Summer Street Bridge, Retrofit, 1995 | MA | Boston (over Fort Point Channel) | MHD | STV Group | Six-span continuous steel beams | LRB (DIS) | AASHTO $A = 0.17g$, Soil profile, Type III |
| West Street over I-93, Retrofit, 1995 | MA | Wilmington | MHD | Vanesse Hangen Brustlin, | Four-span continuous steel beams with concrete deck. | LRB (DIS) | AASHTO $A = 0.17g$, Soil profile, Type I |
| Park Hill over Mass. Pike (I-90), 1995 | MA | Millbury | Mass Turnpike | Purcell Assoc./HNTB | — | EradiQuake (RJ Watson) | — |
| RT 6 Swing Bridge, 1995 | MA | New Bedford | MHD | Lichtenstein | — | EradiQuake (RJ Watson) | — |
| Mass Pike (I-90) over Fuller & North Sts., 1996 | MA | Ludlow | Mass Turnpike | Maguire/HNTB | — | EradiQuake (RJ Watson) | — |
| Endicott Street over RT 128 (I-95), 1996 | MA | Danvers | MHD | Anderson Nichols | — | EradiQuake (RJ Watson) | — |
| I-93 Mass Ave. Interchange, 1996 | MA | S. Boston (Central Artery (I-93)/Tunnel (I-90)) | MHD | Ammann & Whitney | — | HDR (SEP, formerly Furon) | — |
| Holyoke/South Hadley Bridge, 1996 | MA | South Hadley, MA (Reconstruct over Conn. River & Canal St.) | MHD | Bayside Eng. Assoc., Inc. | — | LRB, NRB (SEP, formerly Furon) | — |
| NB I-170 Bridge, New, 1991 | MO | St. Louis (Metrolink Light Rail over NB I-170) | BSDA | Booker Assoc., Inc. and Horner & Shifrin | Two-span cont. steel box girder flanked by short span steel box girders | LRB (DIS/Furon) | AASHTO $A = 0.1g$, Soil profile, Type I |
| Ramp 26 Bridge, New, 1991 | MO | St. Louis (Metrolink Light Rail over Ramp 26) | BSDA | Booker Assoc., Inc. and Horner & Shifrin | Four-span cont. haunched conc. box girder | LRB (DIS/Furon) | AASHTO $A = 0.1g$, Soil profile, Type I |
| Springdale Bridge, New, 1991 | MO | St. Louis (Metrolink Light Rail over Springdale Rd.) | BSDA | Booker Assoc., Inc. and Horner & Shifrin | Three-span cont. haunched conc. box girder | LRB (DIS/Furon) | AASHTO $A = 0.1g$, Soil profile, Type I |
| SB I-170/EB I-70 Bridge, New, 1991 | MO | St. Louis (Metrolink Light Rail over SB I-170/EB I-70) | BSDA | Booker Assoc., Inc. and Horner & Shifrin | Simple span steel box girder, cont. haunched conc. box girder; cont. curved steel box girder | LRB (DIS/Furon) | AASHTO $A = 0.1g$, Soil profile, Type I |

| | | | | | | | |
|---|---|---|---|---|---|---|---|
| Conrail Newark Branch Overpass E106.57, Retrofit, 1994 | NJ | Newark (NJ Tpk. NB over Conrail-Newark Branch) | NJTPA | Gannett-Fleming, Inc. | Steel plate girders, four simple spans | LRB (DIS/Furon) | AASHTO $A = 0.18g$, Soil profile, Type II |
| Wilson Avenue Overpass E105.79SO, Retrofit, 1994 | NJ | Newark (NJ Tpk. Relocated E-NSO & W-NSO over Wilson Ave.) | NJTPA | Frederick R. Harris, Inc. | Steel beams, three simple spans | LRB (DIS/Furon) | AASHTO $A = 0.18g$, Soil profile, Type I |
| Relocated E-NSO Overpass W106.26A, New, 1994 | NJ | Newark (NJ Tpk. E-NSO ramp) | NJTPA | Frederick R = 2E Harris, Inc. | Steel plate girders, cont. units of five and four spans | LRB (DIS/Furon) | AASHTO $A = 0.18g$, Soil profile, Type II |
| Berry's Creek Bridge, Retrofit, 1995 | NJ | E. Rutherford (Rte. 3 over Berry's Cr. and NJ Transit) | NJDOT | Goodkind and O'Dea, Inc. | Cont. steel plate girders; units of three, four, three, and three spans | LRB (Furon) | AASHTO $A = 0.18g$, Soil profile, Type II |
| Conrail Newark Branch Overpass W106.57, Retrofit, 1995 | NJ | Newark (NJ Tpk. Rd. NSW over Conrail-Newark Branch & access rd.) | NJTPA | Frederick R. Harris, Inc. | Steel beams, six simple spans | LRB (DIS) | AASHTO $A = 0.18g$, Soil profile, Type I |
| Norton House Bridge, Retrofit, 1996 | NJ | Pompton Lakes Borough and Wayne Township, Passaic County | NJDOT | A.G. Lichtenstein & Assoc., | Three-span continuous steel beams | LRB (DIS) | AASHTO $A = 0.18g$, Soil profile, Type II |
| Tacony-Palmyra Approaches, 1996 | NJ | Palmyra, NJ | Burlington County Bridge Comm. | Steinman/Parsons Engineers | — | LRB (SEP, formerly Furon) | — |
| Rt. 4 over Kinderkamack Rd., 1996 | NJ | Hackensack, NJ (Widening & Bridge Rehabilitation) | NJDOT | A.G. Lichtenstein & Assoc. | — | LRB, NRB (SEP) | — |
| Baldwin Street/Highland Avenue, 1996 | NJ | Glen Ridge, NJ Bridge over Conrail | NJDOT | A.G. Lichtenstein & Asso. | — | LRB NRB (SEP, formerly Furon) | — |
| I-80 Bridges B764E & W, Retrofit, 1992 | NV | Verdi, Washoe Co. (I-80 over Truckee R. and a local roadway) | NDOT | NDOT | Simple span composite steel plate girders or rolled beams | LRB (DIS/Furon) | AASHTO $A = 0 = 2E37g$, Soil profile, Type I |
| West Street Overpass, Retrofit, 1991 | NY | Harrison, Westchester Co. (West St. over I-95 New England Thwy.) | NYSTA | N.H. Bettigole, P.C. | Four simple span steel beam structures | LRB (DIS/Furon) | AASHTO $A = 0.19g$, Soil profile, Type III |
| Aurora Expressway Bridge, Retrofit, 1993 | NY | Erie Co. (SB lanes of Rte. 400 Aurora Expy. over Cazenovia Cr.) | NYSDOT | NYSDOT | Cont. steel beams with conc. deck | LRB (DIS/Furon) | AASHTO $A = 0.19g$, Soil profile, Type III |
| Mohawk River Bridge, New, 1994 | NY | Herkimer | NYSTA | Steinman Boynton Gronquist & Birdsall | Three-span haunched riveted steel plate girders; simple span riveted steel plate girders or rolled beams | LRB (DIS/Furon) | AASHTO $A = 0.19g$, Soil profile, Type II |

**TABLE 41.5 (continued)** Seismically-Isolated Bridges in North America

| Bridge | Location | | Owner | Engineer | Bridge Description | Bearing Type | Design Criteria |
|---|---|---|---|---|---|---|---|
| Moodna Creek Bridge, Retrofit, 1994 | NY | Orange County (NYST over Moodna Cr. at MP52.83) | NYSTA | Ryan Biggs Assoc., Inc. | Three simple spans; steel plate girder center span; rolled beam side spans | LRB (DIS/Furon) | AASHTO $A = 0.15g$, Soil profile, Type II |
| Conrail Bridge, New, 1994 | NY | Herkimer (EB and WB rdwys. of NYST over Conrail, Rte. 5, etc.) | NYSTA | Steinman Boynton Gronquist & Birdsall | Four-span cont. curved haunched welded steel plate girders. | LRB (DIS/Furon) | AASHTO $A = 0.19g$, Soil profile, Type II |
| Maxwell Ave. over I-95, 1995 | NY | Rye | NYS Thruway Authority | Casler Houser & Hutchison | — | EradiQuake (RJ Watson) | — |
| JFK Terminal One Elevated Roadway, New, 1996 | NY | JFK International Airport, New York City | Port Authority of New York & New Jersey | STV Group | Continuous and simple span steel plate girders | LRB | AASHTO $A = 0.19g$, Soil profile, Type III |
| Buffalo Airport Viaduct, 1996 | NY | Buffalo | NFTA | Lu Engineers | — | EradiQuake (RJ Watson) | — |
| Yonkers Avenue Bridge, 1997 | NY | Yonkers | NY DOT | Voilmer & Assoc. | — | EradiQuake (RJ Watson) | — |
| Clackamas Connector, New, 1992 | OR | Milwaukie (part of Tacoma St. Interchange) | ODOT | ODOT | Eight-span cont=2E post-tensioned conc. trapez. box girder | LRB (DIS/Furon) | AASHTO $A = 0.29g$, Soil profile, Type III |
| Hood River Bridges, 1995 | OR | Hood River, OR | ODOT | ODOT | — | NRB (Furon) | — |
| Marquam Bridge, Retrofit, 1995 | OR | — | ODOT | — | — | FIP | — |
| Hood River Bridge, Retrofit, 1996 | OR | Hood River, OR | ODOT | ODOT | — | FIP | — |
| Toll Plaza Road Bridge, New, 1990 | PA | Montgomery Co. (Approach to toll plaza over Hwy. LR145) | PTC | CECO Assoc., Inc. | 176 ft simple span composite steel plate girder | LRB (DIS/Furon) | AASHTO $A = 0.1g$, Soil profile, Type II |
| Montebella Bridge Relocation, 1996 | PR | Puerto Rico | P.R. Highway Authority | Walter Ruiz & Assoc. | — | LRB, NRB (SEP, formerly Furon) | — |
| Blackstone River Bridge, New, 1992 | RI | Woonsocket | RIDOT | R.A. Cataldo & Assoc. | Four-span cont. composite steel plate girders | LRB (DIS/Furon) | AASHTO $A = 0.1g$, Soil profile, Type II |
| Providence Viaduct, Retrofit, 1992 | RI | Rte. I-95, Providence | RIDOT | Maguire Group | Five-span steel plate girders/hunched steel plate girder units | LRB (DIS/Furon) | AASHTO $A = 0.32g$, Soil profile, Type III |
| Seekonk River Bridge, Retrofit, 1995 | RI | Pawtuckett (I-95 over Seekonk River) | RIDOT | A.G Lichenstein & Assoc. | Haunched steel, two-girder floor beam construction. | LRB (DIS) | AASHTO $A = 0.32g$, Soil profile, Type I |

| | | | | | | | |
|---|---|---|---|---|---|---|---|
| I-295 to Rt. 10, 1996 | RI | Warwick/Cranston (Bridges 662 & 663) | RIDOT | Commowealth Engineers & Consultants | — | LRB (SEP, formerly Furon) | — |
| Chickahominy River Bridge, New, 1996 | VA | Hanover-Hennico County Line (US1 over Chickahominy River) | VDOT | Alpha Corp. | Simple span prestress concrete I-girders with continuous deck. | LRB (DIS) | AASHTO $A = 0.13g$, Soil profile, Type I |
| Ompompanoosuc River Bridge, Retrofit, 1992 | VT | Rte. 5, Norwich | VAT | VAT | Three-span cont. steel plate girders | LRB (DIS/Furon) | AASHTO $A = 0.25g$, Soil profile, Type III |
| Cedar River Bridge New, 1992 | WA | Renton (I-405 over Cedar R. and BN RR) | WSDOT | WSDOT | Four-span cont. steel plate girders | LRB (DIS/Furon) | AASHTO $A = 0.25g$, Soil profile, Type II |
| Lacey V. Murrow Bridge, West Approach, Retrofit, 1992 | WA | Seattle (Approach to orig. Lake Washington Floating Br.) | WSDOT | Arvid Grant & Assoc., Inc. | Cont. conc. box girders; cont. deck trusses; simple span tied arch | LRB (DIS/Furon) | AASHTO $A = 0.25g$, Soil profile, Type II |
| Coldwater Creek Bridge No. 11, New, 1994 | WA | SR504 (Mt. St. Helens Hwy.) over Coldwater Lake Outlet | WSDOT | WSDOT | Three-span cont. steel plate girders | LRB (DIS/Furon) | AASHTO $A = 0.55g$, Soil profile, Type I |
| East Creek Bridge No. 14, New, 1994 | WA | SR504 (Mt. St. Helens Hwy.) over East Cr. | WSDOT | WSDOT | Three-span cont. steel plate girders | LRB (DIS) | AASHTO $A = 0.55g$, Soil profile, Type I |
| Home Bridge, New, 1994 | WA | Home (Key Penninsula Highway over Von Geldem Cove) | Pierce Co. Public Works/Road Dept. | Pierce Co. Public WorksDept. | Prestressed concrete girders; simple spans; continuous for live load. | LRB (DIS) | AASHTO $A = 0.25g$, Soil profile, Type II |
| Duwamish River Bridge, Retrofit, 1995 | WA | Seattle (I-5 over Duwamish River) | WSDOT | Exceltech | Cont. curved steel plate girder unit flanked by curved concrete box girder end spans | LRB (DIS) | AASHTO $A = 0.27g$, Soil profile, Type II |

**TABLE 41.6** Bridges in North America with Supplemental Damping Devices

| Bridge | Location | Type and Number of Dampers | Year | Notes |
|---|---|---|---|---|
| San Francisco–Oakland Bay Bridge | San Francisco, CA | Viscous dampers Total: 96 | 1998 (design) | Retrofit of West Suspension spans. 450~650 kips force output, 6~22 in. strokes |
| Gerald Desmond Bridge | Long Beach, CA | Viscous dampers (Enidine) Total: 258 | 1996 | Retrofit, 258 × 50 kip shock absorbers, 6 in. stroke |
| Cape Girardeau Bridge | Cape Girardeau, MO | Viscous dampers (Taylor) | 1997 | New construction of a cable-stayed bridge; Dampers used to control longitudinal earthquake movement while allowing free thermal movement. |
| The Golden Gate Bridge | San Francisco, CA | Viscous dampers (to be det.) Total: 40 | 1999 (est.) | Retrofit, 40 × 650 kip nonlinear dampers, ± 24 in. |
| Santiago Creek Bridge | California | Viscous dampers (Enidine) | 1997 (est.) | New construction; dampers at abutments for energy dissipation in longitudinal direction |
| Sacramento River Bridge at Rio Vista | Rio Vista, CA | Viscous dampers (Taylor) | 1997 (est.) | Retrofit; eight dampers used to control uplift of lift-span towers |
| Vincent Thomas Bridge | Long Beach, CA | Viscous dampers (to be det.) Total: 16 | — | Retrofit, 8 × 200 kip and 8 × 100 kip linear dampers, ± 12 in. |
| Montlake Bridge | Seattle, WA | Viscous dampers (Taylor) | 1996 | Protection of new bascule leafs from runaway |
| West Seattle Bridge | Seattle, WA | Viscous dampers (Taylor) | 1990 | Deck isolation for swing bridge. |

## 41.7 Summary

An attempt has been made to introduce the basic concepts of seismic isolation and supplemental energy dissipation, their history, current developments, applications, and design-related issues. Although significant strides have been made in terms of implementing these concepts to structural design and performance upgrade, it should be mentioned that these are emerging technologies and advances are being made constantly. With more realistic prototype testing results being made available to the design community of seismic isolation and supplemental energy dissipation devices from the FHWA/Caltrans testing program, significant improvement in code development will continuously make design easier and more standardized.

## Acknowledgments

The author would like to express his deepest gratitude to Professor T. T. Soong, State University of New York at Buffalo, for his careful, thorough review, and many valuable suggestions. The author is also indebted to Dr. Lian Duan, California State Department of Transportation, for his encouragement, patience, and valuable inputs.

## References


1. Applied Technology Council, *Improved Seismic Design Criteria for California Bridges: Provisional Recommendations*, ATC-32, Applied Technology Council, Redwood City, 1996.
2. Housner, G. W., Bergman, L. A., Caughey, T. K., Chassiakos, A. G., Claus, R. O., Masri, S. F., Sekelton, R. E., Soong, T. T., Spencer, B. F., and Yao, J. T. P., Structural control: past, present, and future, *J. Eng. Mech. ASCE,* 123(9), 897–971.
3. Soong, T. T., and Gargush, G. F., Passive energy dissipation and active control, in *Structure Engineering Handbook*, Chen, W. F., Ed., CRC Press, Boca Raton, FL, 1997.
4. Soong, T. T. and Gargush, G. F., *Passive Energy Dissipation Systems in Structural Engineering*, John Wiley & Sons, New York, 1997.
5. Housener, G. W. and Jennings, P. C., *Earthquake Design Criteria*, Earthquake Engineering Research Institute, 1982.
6. Newmark, N. M. and Hall, W. J., Procedures and Criteria for Earthquake Resistant Design, *Building Practice for Disaster Mitigation*, Department of Commerce, Feb. 1973.
7. Dynamic Isolation Systems, *Force Control Bearings for Bridges — Seismic Isolation Design*, Rev. 4, Lafayette, CA, Oct. 1994.
8. Clough, R. W. and Penzien, J., *Dynamics of Structures*, 2nd ed., McGraw-Hill, New York, 1993.
9. Zhang, R., Soong, T. T., and Mahmoodi, P., Seismic response of steel frame structures with added viscoelastic dampers, *Earthquake Eng. Struct. Dyn.*, 18, 389–396, 1989.
10. Earthquake Protection Systems, *Friction Pendulum Seismic Isolation Bearings*, Product Technical Information, Earthquake Protection Systems, Emeriville, CA, 1997.
11. Liu, D. W, Nobari, F. S., Schamber, R. A., and Imbsen, R. A., Performance based seismic retrofit design of Benicia–Martinez bridge, in *Proceedings, National Seismic Conference on Bridges and Highways,* Sacramento, CA, July 1997.
12. Constantinou, M. C. and Symans, M. D., Seismic response of structures with supplemental damping, *Struct. Design Tall Buildings*, 2, 77–92, 1993.
13. Ingham, T. J., Rodriguez, S., Nader, M. N., Taucer, F, and Seim, C., Seismic retrofit of the Golden Gate Bridge, in *Proceedings, National Seismic Conference on Bridges and Highways,* Sacramento, CA, July 1997.
14. Taylor Devices, *Sample Technical Specifications for Viscous Damping Devices*, Taylor Devices, Inc., North Tonawanda, NY, 1996.
15. Lin, R. C., Liang, Z., Soong, T. T., and Zhang, R., An Experimental Study of Seismic Structural Response with Added Viscoelastic Dampers, Report No. NCEER-88-0018, National Center For Earthquake Engineering Research, State University of New York at Buffalo, February, 1988.
16. Crosby, P., Kelly, J. M., and Singh, J., Utilizing viscoelastic dampers in the seismic retrofit of a thirteen story steel frame building, *Structure Congress,* XII, Atlanta, GA, 1994.
17. Skinner, R. I., Kelly, J. M., and Heine, A. J., Hysteretic dampers for earthquake resistant structures, *Earthquake Eng. Struct. Dyn.*, 3, 297–309, 1975.
18. Pall, A. S. and Pall, R., Friction-dampers used for seismic control of new and existing buildings in canada, in *Proceedings ATC 17-1 Seminar on Isolation, Energy Dissipation and Active Control,* San Francisco, CA, 1992.
19. AASHTO, *Guide Specifications for Seismic Isolation Design*, American Association of State Highway and Transportation Officials, Washington, D.C., June 1991.
20. FEMA, NEHRP Recommended Provisions for Seismic Regulations for New Buildings, 1994 ed., Federal Emergency Management Agency, Washington, D.C., May 1995.
21. EERC/Berkeley, Pre-qualification Testing of Viscous Dampers for the Golden Gate Bridge Seismic Rehabilitation Project, A Report to T. Y. Lin International, Inc., Report No. EERCL/95-03, Earthquake Engineering Research Center, University of California at Berkeley, December 1995.

22. AASHTO, *Standard Specifications for Highway Bridges*, 16th ed., American Association of State Highway and Transportaion Officials, Washington, D.C., 1996.
23. Priestley, M. J. N, Seible, F., and Calvi, G. M., *Seismic Design and Retrofit of Bridges*, John Wiley an&& Sons, New York, 1996.
24. Whittaker, A., Tentative General Requirements for the Design and Construction of Structures Incorporating Discrete Passive Energy Dissipation Devices, ATC-15-4, Redwood City, CA, 1994.
25. Applied Technology Council, BSSC Seismic Rehabilitation Projects, ATC-33.03 (Draft), Redwood City, CA, .
26. AASHTO-T3 Committee Task Group, *Guide Specifications for Seismic Isolation Design,* T3 Committee Task Group Draft Rewrite, America Association of State Highway and Transportation Officials, Washington, D.C., May, 1997.